

Large-Eddy Simulations of Magnetohydrodynamic Turbulence in Heliophysics and Astrophysics

Mark Miesch¹ · William Matthaeus² · Axel Brandenburg³ · Arakel Petrosyan^{4,5} · Annick Pouquet^{6,7} · Claude Cambon⁸ · Frank Jenko⁹ · Dmitri Uzdensky¹⁰ · James Stone¹¹ · Steve Tobias¹² · Juri Toomre¹³ · Marco Velli¹⁴

Received: 15 April 2015 / Accepted: 17 July 2015 / Published online: 31 July 2015
© Springer Science+Business Media Dordrecht 2015

Abstract We live in an age in which high-performance computing is transforming the way we do science. Previously intractable problems are now becoming accessible by means of increasingly realistic numerical simulations. One of the most enduring and most challenging of these problems is turbulence. Yet, despite these advances, the extreme parameter regimes encountered in space physics and astrophysics (as in atmospheric and oceanic physics) still preclude direct numerical simulation. Numerical models must take a Large Eddy Simulation

✉ M. Miesch
miesch@ucar.edu

W. Matthaeus
whm@udel.edu

A. Brandenburg
brandenb@nordita.org

A. Petrosyan
a.petrosy@iki.rssi.ru

A. Pouquet
pouquet@ucar.edu

C. Cambon
claude.cambon@ec-lyon.fr

F. Jenko
jenko@physics.ucla.edu

D. Uzdensky
Uzdensky@colorado.edu

J. Stone
jstone@astro.princeton.edu

J. Toomre
jtoomre@lcd.colorado.edu

M. Velli
mveli@jpl.nasa.gov

¹ HAO/NCAR, 3080 Center Green Dr., Boulder, CO 80301, USA

² Dept. of Physics and Astronomy, University of Delaware, Newark, DE 19716, USA

(LES) approach, explicitly computing only a fraction of the active dynamical scales. The success of such an approach hinges on how well the model can represent the subgrid-scales (SGS) that are not explicitly resolved. In addition to the parameter regime, heliophysical and astrophysical applications must also face an equally daunting challenge: magnetism. The presence of magnetic fields in a turbulent, electrically conducting fluid flow can dramatically alter the coupling between large and small scales, with potentially profound implications for LES/SGS modeling. In this review article, we summarize the state of the art in LES modeling of turbulent magnetohydrodynamic (MHD) flows. After discussing the nature of MHD turbulence and the small-scale processes that give rise to energy dissipation, plasma heating, and magnetic reconnection, we consider how these processes may best be captured within an LES/SGS framework. We then consider several specific applications in heliophysics and astrophysics, assessing triumphs, challenges, and future directions.

Keywords Turbulence · Magnetohydrodynamics · Simulation

1 Introduction

On May 20–23, 2013 a workshop was held at the National Center for Atmospheric Research (NCAR) in Boulder, Colorado, USA entitled “Large-Eddy Simulations (LES) of Magnetohydrodynamic (MHD) Turbulence.” The workshop was sponsored by NCAR’s Geophysical Turbulence Program (GTP) and involved approximately fifty participants from eight countries.

This review paper is a product of the GTP workshop, though it is not intended as a comprehensive account of the proceedings. Rather, it is intended as a summary of the issues addressed and the insights achieved, as well as an inspiration and a guide to promote future work on this subject. Though the subject of interest, namely LES of MHD turbulence,

³ NORDITA, KTH Royal Inst. Tech. and Stockholm Univ., Roslagstullsbacken 23, 10691 Stockholm, Sweden

⁴ Space Research Inst., Russian Academy of Sciences, Profsoyuznaya 84/32, Moscow, Russia

⁵ Moscow Institute of Physics and Technology (State University), 9 Institutskiy per., Dolgoprudny, Moscow Region 141700, Russia

⁶ NCAR, P.O. Box 3000, Boulder, CO 80307, USA

⁷ Dept. of Applied Math., Univ. of Colorado, Boulder, CO 80309-256, USA

⁸ Laboratoire de Mécanique des Fluides et d’Acoustique, École Centrale de Lyon, 36, av., Guy de Collongues, 69134 Ecully cedex, France

⁹ Dept. of Physics and Astronomy, UCLA, 475 Portola Plaza, Office 4-720 PAB, Box 951547, Los Angeles, CA 90095-1547, USA

¹⁰ CIPS, Physics Dept., UCB-390, Univ. Colorado, Boulder, CO 80309-0390, USA

¹¹ Dept. of Astrophysical Sciences, Princeton Univ., Peyton Hall, Ivy Lane, Princeton, NJ 08544-1001, USA

¹² Dept. of Applied Mathematics, University of Leeds, Leeds, LS2 9JT, UK

¹³ JILA and Dept. of Astrophysical and Planetary Sciences, Univ. of Colorado, Boulder, CO 80309-0440, USA

¹⁴ Jet Propulsion Laboratory, California Inst. Tech., Pasadena, CA 91109-8099, USA

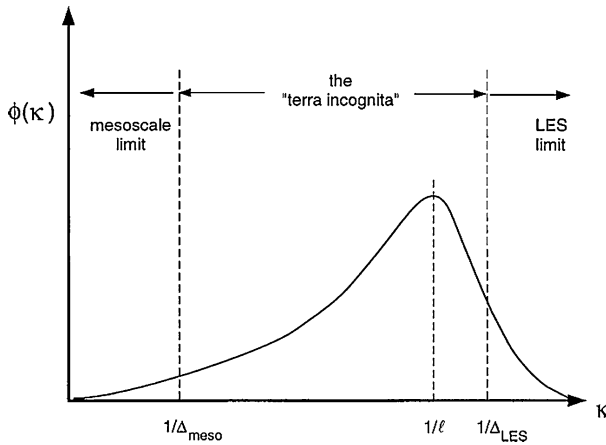


Fig. 1 The “Terra Incognita” and the realm of LES (from Wyngaard 2004, presented at the workshop by Peter Sullivan). Shown is an idealized power spectrum of some turbulent field ϕ as a function of wavenumber κ (referred to elsewhere in the paper as k). The peak of the spectrum lies at $\kappa \sim 1/\ell$ where ℓ is a characteristic length scale of the turbulence. If the grid spacing of the simulation, Δ is much larger than ℓ , then the turbulence is entirely unresolved, defining the so-called mesoscale limit of atmospheric science ($\Delta \geq \Delta_{\text{meso}}$). If the turbulence is partially resolved, capturing the peak in the spectrum but not the viscous dissipation scale ℓ_d ($\ell_d \leq \Delta \leq \ell$), then this is the appropriate scenario for LES

is ostensibly rather specific, it encompasses a number of subtle physical processes and diverse applications and it draws on the formidable discipline of efficient numerical algorithm development on high-performance computing architectures.

The fundamental challenge that defines the field of LES is that the range of dynamical scales active in many turbulent fluid systems far exceeds the range that can be explicitly captured in a computer simulation. Examples include the convection zones of stars, planetary atmospheres, astrophysical accretion disks, and industrial applications such as gas turbines. The *central premise* of LES is that large scales dominate the turbulent transport and energy budget so a numerical simulation that captures those scales explicitly will provide a realistic depiction of the flow for all practical purposes, provided that the small scales that cannot be resolved are somehow taken into account. Strategies for incorporating the small scales include explicit subgrid-scale (SGS) models or implicit numerical dissipation schemes.

The range of validity for LES is illustrated schematically in Fig. 1. Consider a numerical simulation of a turbulent fluid system in which the turbulent energy spectrum peaks at some characteristic wavenumber ℓ^{-1} . Due to the nature of digital computing, any such simulation can only capture a finite range in wavenumber, say from L^{-1} to Δ^{-1} . Guided by the *central premise* stated above, the lower bound of this wavenumber range often corresponds to the largest scales in the system $L > \ell$. Meanwhile, the higher bound in wavenumber is determined by the resolution limit Δ which may correspond to a numerical grid spacing or to the effective width of some explicit low-pass filtering operation that averages over the smaller scales (Sect. 4).

If the resolution limit Δ is smaller than the viscous, thermal, and magnetic dissipation scales, collectively represented here as ℓ_{diss} , then the simulation may be regarded as a direct numerical simulation (DNS). However, as noted above, DNS are not possible for most turbulent systems in astrophysics and space physics. A much more tractable situation is when the resolution limit captures the turbulence scale ℓ but not the dissipation scales; $\ell_{\text{diss}} \ll \Delta \ll \ell$. This is the realm of LES. Here SGS models can exploit the self-similarity of the turbulent

cascade in the inertial range and diffusive prescriptions are often sufficient (although even that may not be true in MHD). Ideally, the grid spacing Δ should also be much less than other scales that lead to large-scale anisotropy, such as the Rossby deformation radius, the Bolgiano scale of convection, and the pressure and density scale heights. When this is not possible, such sources of anisotropy must be taken into account in any explicit SGS model.

Sometimes the characteristic scale of a turbulent flow component is smaller than the effective resolution of the simulation or model $\ell < \Delta$. One may then model the influence of the unresolved scales on mean, resolved flows but one might not refer to this as an LES model. A better terminology might be to call this a Reynolds-Averaged Navier-Stokes (RANS) approach with some model for the turbulent transport, possibly including non-diffusive as well as diffusive components. In the following, such calculations are also referred to as mean-field simulations (MFS).

If properly formulated, the LES approach should converge to the DNS approach as Δ goes to zero. This is not necessarily true for RANS. For many systems such as homogeneous turbulence, there is a smooth transition from RANS to LES as the filter scale is decreased from $\Delta > \ell$ to $\Delta \ll \ell$ (Schmidt 2015). SGS models may include non-diffusive transport that resembles the Reynolds stress modeling in a RANS system, blurring the distinction between the two approaches. Numerical models of such systems may lie anywhere along a continuous spectrum of modeling approaches from RANS to LES to DNS. On the RANS end of the spectrum, the reliability of the Reynolds stress model is paramount, along with analogous prescriptions for turbulent heat transport and, in the MHD case, turbulent magnetic induction. For LES models that lie more toward the DNS end of the spectrum the details of the SGS model presumably become less important, though the simulation becomes more sensitive to the accuracy of the numerical algorithm. Also, as one moves across the spectrum from RANS to LES to DNS the computational cost increases greatly, along with the number of degrees of freedom.

In other systems, the transition from RANS to LES is less straightforward; one must beware of the “Terra Incognita” that may lie between (Fig. 1). As the LES filter size Δ approaches ℓ , SGS models that rely on the self-similar nature of turbulent cascades may break down. There may be a maximum scale $\Delta_{LES} < \ell$ above which the filtering procedure becomes ill defined and unreliable. On the other hand, RANS models may require a sufficient scale separation to make statistical averages meaningful, such that $\Delta \gg \ell$. In Fig. 1 this minimum scale for the validity of RANS is labelled as Δ_{meso} , in reference to the mesoscale modeling of the Earth’s atmosphere. In between these two limits, $\Delta_{LES} < \Delta < \Delta_{meso}$, lies the Terra Incognita where turbulence modeling and simulation can become much more challenging (Wyngaard 2004).

Due largely to the industrial and atmospheric applications, LES of hydrodynamic turbulence is widespread and relatively mature (Sagaut 2006). However, most astrophysical and geophysical flows of interest are electrically conducting plasmas in which the magnetic field plays an essential dynamical role. For these flows, models must take magnetism into account either through the kinetic theory of plasmas (generally necessary for the smallest scales) or through the simplifying equations of MHD (often well justified for large scales). Though LES of MHD turbulence can build upon the large body of work in hydrodynamic (HD) turbulence, it poses unique challenges that must be addressed specifically. These include small-scale anisotropy, nonlocal spectral transfer, and magnetic reconnection.

In Sect. 2 we discuss some of these unique challenges of MHD turbulence and highlight particular features of MHD turbulence that may promote the development of reliable SGS models. In Sect. 3 we consider the physics of the smallest scales where ideal MHD no longer applies, promoting mechanical and magnetic energy dissipation and magnetic reconnection,

and we ask how these scales may influence the dynamics of the large scales. We then review current SGS modeling approaches for MHD in Sect. 4 and assess the triumphs and tribulations of current applications in Sect. 5. We summarize the state of the field in Sect. 6 and anticipate where it may be headed in the future.

Though many of the physical processes and challenges we address have implications throughout astrophysics, we will focus primarily on solar and space physics in this review. This is done to allow us to achieve some depth in the material covered while still maintaining a manageable length. For a more comprehensive overview of LES/SGS in astrophysics the reader is referred to Schmidt (2015).

2 MHD Turbulence: Challenges and Building Blocks

2.1 Anisotropy in Incompressible Unbounded Turbulence, from HD to MHD

Global anisotropy is an essential feature of MHD flows, particularly in the presence of a mean magnetic field. The existence of a unique fixed orientation yields breaking isotropy towards axisymmetry, with or without mirror symmetry. System rotation, buoyancy, and density stratification further contribute to global anisotropy and inhomogeneity as in HD turbulence. However, in these HD cases, if one considers scales small enough (e.g. much smaller than the Rossby radius of deformation for rotation) then the constraints become negligible. For MHD turbulence the situation is exactly the opposite; the flow never “forgets” the existence of the large-scale constraint imposed by the magnetic field. Indeed as one goes to smaller and smaller scales the anisotropy increases (Tobias et al. 2013). This is a severe constraint that must be respected by sub-grid scale models.

In the absence of a mean magnetic field, Alfvénic MHD turbulence can be investigated with a more (Iroshnikov 1963) or less (Kraichnan 1965) isotropized model. However, even in this case, the substructure of Alfvén wave packets at small scales cannot be ignored in the overall structure and dynamics of the turbulence. If the governing orientation of the small-scale Alfvén packets is seen as random, a sophisticated stochastic model, mixing anisotropy and intermittency, is needed (one such model was discussed by W. Matthaeus at the workshop). Again, this is a formidable challenge facing SGS in MHD.

The theory for MHD turbulence has been developed over the past few decades, and there are many recent reviews summarizing various aspects (Kraichnan and Montgomery 1980; Biskamp 2003; Zhou et al. 2004; Petrosyan et al. 2010; Brandenburg and Nordlund 2011; Tobias et al. 2013). One familiar phenomenology is that of interacting wavepackets. This phenomenology arises because nonlinear Alfvén waves are exact solutions of the full incompressible MHD equations (see, e.g. Parker 1979). A more precise statement is that nonlinear interactions only take place when oppositely-signed Elsässer fields $\mathbf{Z}_+ = \mathbf{v} + \mathbf{b}$ and $\mathbf{Z}_- = \mathbf{v} - \mathbf{b}$ overlap in space, this statement being valid with or without a mean magnetic field \mathbf{B}_0 , and even in two-dimensional geometry with $\mathbf{B}_0 = 0$ where there is no global propagation direction at all. In any case one often encounters the heuristic explanation that interactions only take place when oppositely propagating wave-packets interact with each other. When coherent propagation can occur, it anisotropically interferes with nonlinearity, and gives rise to anisotropic spectra (Shebalin et al. 1983; Oughton et al. 1994). A related effect, the dynamic alignment of turbulent velocity and magnetic fields, also has strong effects on MHD turbulence. Global dynamic alignment may occur in some ranges of parameter space (Dobrowolny et al. 1980; Ting et al. 1986; Stribling and Matthaeus 1991; Stawarz et al. 2012) as a form of long time turbulent relaxation. However local dynamic alignment

(Milano et al. 2001; Boldyrev 2006; Matthaeus et al. 2008a) occurs rapidly in turbulence. Other types of local relaxation that reduce or suppress the strength of nonlinearities imply formation of local patches of correlation associated with Beltrami velocity fields and force-free magnetic fields (Servidio et al. 2008). Numerical experiments also seem to indicate that the degree of alignment of field and velocity is scale-dependent, with the alignment variation even propagating into the dissipative regime (Boldyrev 2006; Mason et al. 2006).

For MHD turbulence with a strong externally supported DC magnetic field \mathbf{B}_0 , it is possible to form a large-scale condensate of energy which influences the turbulent cascade at all smaller scales (Dmitruk and Matthaeus 2009). Condensation, whether of this type, or of the inverse cascade type, may be associated with generation of low frequency $1/f$ noise and long time correlations and sporadic level changes of energy and other quantities over very long times (Dmitruk and Matthaeus 2007). All of these dynamical effects may influence computed solutions, and should be respected by appropriate sub-grid scale models. These factors, which present a formidable challenge for SGS prescriptions, are discussed in more detail in Sect. 3.

It is possible to describe the second-order correlation tensors with a minimal number of correlators, as scalar or pseudo-scalar spectra, accounting for the solenoidal properties of both velocity and vorticity fields. The seminal studies by Robertson (1940), Chandrasekhar (1950, 1951), Batchelor (1982), and Craya (1958) were completed by Oughton et al. (1997) in the MHD case. Developed independently by Cambon's team, a similar formalism improved the decomposition in terms of energy, helicity and especially *polarization* spectra, using the orthonormal bases for solenoidal fields, known as a Craya-Herring frame of reference (Herring 1974), with its variant of helical modes (Cambon and Jacquin 1989; Waleffe 1992). This formalism is discussed at length, with application to turbulence subjected to rotation, density-stratification and uniform shear in the recent monograph by Sagaut and Cambon (2008), and extended to the MHD case by Cambon and collaborators (Favier et al. 2012; Cambon et al. 2012). In addition to the definition of the basic set of spectra and co-spectra, dynamical equations can be written for the correlators, generalizing the Lin equation in isotropic turbulence.

Unfortunately, very few of these results (for both HD and MHD) have been used in recent pseudo-spectral DNS in triple-periodic boxes, even if they could reproduce anisotropic homogeneous turbulence, despite the finite-box effects, standard discretization, questionable ergodicity from a single realization, and other differences with the theoretical context of homogeneous unbounded turbulence. As a first example, helicity cannot be disentangled from directional anisotropy (e.g. angle-dependent, or two-component, energy spectrum) and polarization anisotropy in DNS started with a single realization, e.g. with ABC artificial helical forcing (Salhi et al. 2014). On the other hand, angle-dependent spectra and co-spectra, which are not provided by these recent DNS, are useful to *quantitatively* characterize different anisotropic properties, as the horizontal layering in stably-stratified turbulence, and the opposite trend to generate columnar structures in flows dominated by system rotation. Such structures are often shown only on snapshots in recent DNS, with very indirect linkage to statistical indicators, such as one-component, in terms of wavevector modulus k or transverse wavevector k_{\perp} , spectra. Might there be some analogy between the layering in stably stratified turbulence (which is linked to the kinetic energy cascade of the toroidal velocity component and angle-dependent spectra) and the formation of thin current sheets in MHD, as seen in high-resolution DNS?

In addition, the distinction between the 2D 'vortex' modes and 'rapid' inertial modes is dependent on discretization in conventional pseudo-spectral DNS for purely rotating turbulence, and the dynamics is affected by finite-box effects. Only the use of actual confinement,

as with rigid boundaries, allows one to identify the 2D mode as a dominant one, whereas it is only a marginal limit of inertial wave modes in a very large box, and treated as an integrable singularity in wave turbulence theory (Bellet et al. 2006). Extension of inertial wave turbulence theory, with coupling to ‘actual’ 2D modes, was recently achieved in a rotating ‘slab’ by Scott (2014).

An important question, useful for SGS modeling in LES, is the range of penetration of anisotropy towards smallest scales (see also Sect. 3.2). In the HD case, an external effect such as mean shear firstly affects the largest scales, generating both energy (production) and anisotropy. As suggested by Corrsin (1958), isotropy can be recovered at a typical wavenumber, expressed in terms of mean shear rate S and the dissipation rate ε : $k_S = \sqrt{S^3/\varepsilon}$. Similar threshold wavenumbers were proposed by Ozmidov (1965) for stably-stratified turbulence, replacing S by the Brunt-Väisälä frequency, N , and by Zeman (1994) in rotating turbulence, replacing S by system vorticity. Even if these simple dimensional considerations are only partly supported by DNS or experiments (Lamriben et al. 2011; Delache et al. 2014), they are not sufficient to close the problem and to say that anisotropy can be generally neglected at small scale in HD turbulence, in contrast with MHD turbulence. Rotating turbulence and stably stratified turbulence are much more subtle, because there is no direct production of kinetic energy by the Coriolis force, and no direct production of total energy, kinetic + potential, by the buoyancy force with stabilizing mean density gradient (in contrast with turbulence subjected to mean shear). On the other hand, a scale-by-scale analysis of the anisotropy in rotating turbulence, without artificial forcing, reveals that the anisotropy first increases with increasing wave-number, so that it can be maximum at the smallest scales if the “Zeman wavenumber” $k_\Omega = \sqrt{\Omega^3/\varepsilon}$ is larger than the viscous cutoff. These considerations suggest a refined comparison between inertial wave turbulence theory and weak MHD Alfvénic turbulence, with the latter reviewed and updated by Boldyrev in the GTP workshop (see Tobias et al. 2013).

2.2 Is There a Need for Including Advanced Backscatter Modeling?

In HD turbulence, backscatter to larger scales plays energetically a significant role, but it is usually not systematically correlated with large-scale properties of the flow. On the other hand, at least in helical MHD, backscatter plays a dramatic role in that it is responsible for the generation of magnetic energy at the largest scale through what is known as the α effect. The α effect plays therefore an important role in mean-field simulations (MFS), but is ignored in LES.

The α -effect is linked to the upscale transfer of magnetic helicity, which occurs in helical MHD turbulence through local (inverse cascade) or nonlocal (α -effect) spectral interactions (Pouquet 1996; Seehafer 1996; Brandenburg 2001; Müller et al. 2012). Spectral transfer of cross helicity $\langle \mathbf{u} \cdot \mathbf{B} \rangle$ can also couple large and small scales and should be taken into account in SGS models, as emphasized in the GTP workshop by Yokoi (2013).

Indeed, cross helicity is produced in the presence of gravity \mathbf{g} and a parallel magnetic field \mathbf{B} , giving rise to a pseudo-scalar $\mathbf{g} \cdot \mathbf{B}$ that is odd in the magnetic field, just like the cross helicity (Rüdiger et al. 2011). In such a case, a large-scale magnetic pattern emerges, as can be seen from power spectra and images shown in Fig. 2. Whether or not this large-scale pattern is a result of some inverse cascading of cross helicity, analogous to the α -effect, remains an open question; see Brandenburg et al. (2014) for details.

Another potential mechanism that may contribute the generation of large-scale structure in MHD flows such as that shown in Fig. 2 is the suppression of small-scale turbulent pressure by a large-scale magnetic field. This is currently gaining attention within the context of

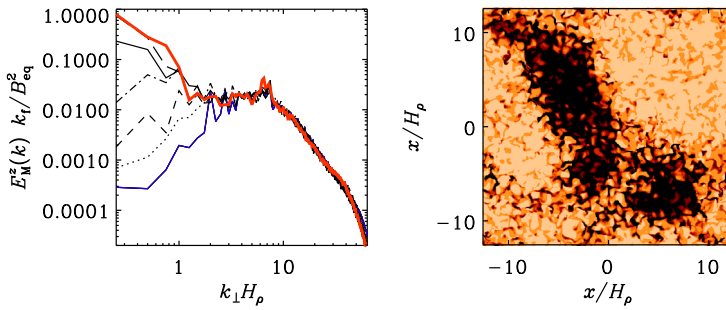


Fig. 2 *Left:* Normalized energy spectra of B_z from an isothermally stratified, randomly forced DNS with $g/c_s^2 k_f = 4$ (sound speed c_s and forcing wavenumber k_f) at turbulent diffusive times ≈ 0.2 (blue line), 0.5, 1, 2, 5, 10, and 20 (red line). *Right:* Magnetic field configuration at the upper surface near the end of the simulation. Adapted from Brandenburg et al. (2014)

mean-field modeling of the Reynolds and Maxwell stresses. If this suppression dominates over the direct contribution of the magnetic pressure, as is the case for fully developed turbulence, then the net effect will be negative (Kleeorin et al. 1989; Rogachevskii and Kleeorin 2007). In a strongly stratified layer, this can lead to an instability, which is now called the negative effective magnetic pressure instability (NEMPI). It has been suggested that NEMPI may play a role in causing the magnetic field to form flux concentrations in the upper regions of the solar convection zone, where the stratification is strongest (Brandenburg et al. 2012; Käpylä et al. 2012; Kemel et al. 2013). Again, this effect has been successfully captured in MFS, where its predictive capabilities have been instrumental in furthering our theoretical understanding. We need to ask whether or not LES should be modified to include this effect, or whether LES are naturally able to capture this type of physics. For example, the dynamic Smagorinsky model used in simulations of stellar convective dynamos by Nelson et al. (2011, 2013) promotes the generation of coherent flux structures by nonlinear feedbacks that are roughly analogous to those responsible for the NEMPI.

2.3 Possible Consequences of Misrepresenting the Small Scales

A practical goal of LES is clearly to keep the code stable. This means that close to the grid scale the flow must become smooth. In reality, the opposite is the case: turbulent diffusion of mean flows, mean magnetic fields, mean temperature, and mean passive scalars decreases with scales. This picture is quite clear in mean-field theory, where turbulent transport coefficients such as magnetic diffusivity, η_t , and α effect are known to become wavenumber-dependent. We do not yet know whether this plays an important role in LES, but we must ask whether certain discrepancies between LES and astrophysical reality can be explained by such shortcomings. Below we discuss one such example.

Realistic global dynamo simulations have revealed that magnetic cycles are possible at rotation rates somewhat faster than the Sun (Brown et al. 2011). Yet, the Sun is known to undergo cycles. Could this be a consequence of misrepresenting the small scales in the simulations?

To approach this question, we need to know what is the governing non-dimensional parameter that determines the transition from cyclic to non-cyclic dynamos. This is a difficult question, because the mechanism behind the solar dynamo is not conclusively identified. Broadly speaking, there are flux transport dynamos where meridional circulation plays an

important role determining the cycle time and migration of magnetic activity belts. The other candidate is just α effect and differential rotation, giving rise to an α - Ω dynamo in which meridional circulation is unimportant. In mean-field theory, the relative importance of the Ω effect for both scenarios is determined by the non-dimensional quantity $C_\Omega = \Delta\Omega/\eta_t k^2$. Here η_t is a measure of the turbulent kinetic energy so C_Ω may be regarded as equivalent to a Rossby number based on the differential rotation. The relative importance of the Ω effect over the α effect depends on the ratio of C_Ω and a similar parameter $C_\alpha = \alpha/\eta_t k$ that characterizes the strength of the α effect. Both C_Ω and the ratio C_Ω/C_α would be underestimated in an LES in which $\eta_t(k)k$ and $\alpha(k)$ are too big, so this suggests that one would need to compensate for this shortcoming by increasing Ω to recover cyclic dynamo action.

Though this reasoning is generally robust, it is based on kinematic mean-field theory so its application to MHD LES must be made with care. For example, MHD/LES convection simulations by Brown et al. (2011) and Nelson et al. (2013) demonstrated a transition from steady to cycling dynamos with both an increase in Ω and a decrease in the SGS component of the turbulent magnetic diffusivity, η_t . This appears to be consistent with the mean-field arguments in the preceding paragraph. However, when the SGS diffusion was decreased in the latter case (Nelson et al. 2013), the kinetic energy of the convection increased and the differential rotation weakened due to Lorentz force feedbacks, implying an effective *decrease* in C_Ω for the cyclic case. Furthermore, though the total magnetic energy was greater in the cyclic, low-dissipation case, the magnetic topology was more complex, with less energy in the mean (axisymmetric) fields. This implies a relatively inefficient α -effect. Further analysis confirmed that despite the relatively weak $\Delta\Omega$ in the cyclic simulation, the primary source of toroidal flux was indeed the Ω -effect, implying $C_\Omega/C_\alpha > 1$.

3 Small-Scale Dynamics: Dissipation, Reconnection and Kinetic Effects

LES methods as applied to HD have as a central goal the ability to compute the dynamics of the resolved scales more accurately under conditions in which the Reynolds numbers are too high for a fully resolved DNS computation. Additional goals may be to compute the direct influence of the unresolved scales on the resolved scales (backscatter), or, in the so-called energy equation approach, to track the transport of unresolved turbulence. Specific formulations of LES relevant to the MHD case will be discussed in more detail in the following section. The complications that MHD introduces into small scale physics become even more challenging when MHD models are employed to approximate the dynamics of a low collisionality (or “kinetic”) plasma. These issues carry over into additional challenges for LES/SGS modeling.

In MHD the dissipation function (for simple resistivity and viscosity) is known, as in HD. However the phenomenology of MHD dissipation is more complex given that both current density structures and vorticity structures are available as sites of enhanced heating. Simulations have shown that this leads to a dependence of the ratio of kinetic to magnetic energy dissipation on the magnetic Prandtl number (Brandenburg 2009, 2011, 2014), which is generally not reproduced by LES.

Not only is there an additional channel for dissipation, but the nonlinear transfer of energy between velocity and magnetic field is known to be more nonlocal in scale than the transfer of total energy across scale (Verma 2004; Alexakis et al. 2005). The possibility that these effects come into play in varying proportions for MHD flows in differing parameter regimes is not only possible but likely, given for example the well known differences in small-scale dynamics in the kinematic dynamo regime, the Alfvénic turbulence regime, and the large

scale reconnection regime. These differences reflect the degree of nonuniversality inherent in MHD behavior, which has been demonstrated in a number of recent studies (Lee et al. 2010; Wan et al. 2012b)

Variability in the nature of the cascade represents a challenge in developing LES for MHD since the correct modeling of important sub-grid scale physics may be situation-dependent. However the challenge is even deeper in the context of low collisionality astrophysical plasmas, even if MHD represents an accurate model at the larger scales. At the smaller scales, comparable to ion gyroscopes or inertial scales, one expects MHD to break down and give way to a more complete dynamical description, which is commonly referred to as the kinetic plasma regime. Processes occurring at the kinetic scales may resemble analogous MHD processes, but may also differ significantly in their detail. The LES developer in such cases may need to understand carefully whether the relevant processes to be incorporated into sub grid scale modeling remain MHD-like, or if they are possibly influenced strongly by kinetic physics.

Two examples of processes that are potentially influenced by kinetic physics are dissipation of fluctuation energy and magnetic reconnection. These processes may lead for example, to electron/ion heating and nonthermal particle acceleration. In many space and astrophysical applications of MHD, from the solar wind to black hole accretion disks, these mechanisms can play a crucial role for the global dynamics of the system, coupling microscopic and macroscopic scales.

One may also ask how the details of small scale processes might have influence on the large-scale dynamics that is the emphasis of LES. As long as the focus remains in the MHD range of scales, in the usual way one may anticipate that energy transfer across scales will be almost independent of scale at high Reynolds number. If an accurate estimation of the energy flux is available, it enables closure of the SGS problem before the dissipative scales are even encountered. This is a key step in the de Karman and Howarth (1938) similarity decay hypothesis, and is a familiar component of most HD LES. Even the MHD models can become more elaborate, for example when there is a need to include backscatter effects (as discussed above). Furthermore, for situations that permit inverse cascade¹ this additional complexity in modeling energy transfer becomes mandatory. However when MHD models are employed for long wavelength description of kinetic plasma behavior, it transpires that there are additional motivations for study of small scale effects in building LES models. These potentially include:

- (i) the requirement of following magnetic topology and connectivity, which may be influenced by small-scale processes such as magnetic reconnection, as well as diffusive effects such as Field Line Random Walk (FLRW);
- (ii) the requirement of computing test particle scattering and/or acceleration, in order to employ the models for study of suprathermal particles, heat conduction or energetic particles such as cosmic rays and solar energetic particles;
- (iii) the requirement of representing dissipation, heating and more complex kinetic responses (including in some cases radiative cooling), which may be regulated by the LES fields.

In each of the above problems the large scale MHD fields and the cascade that they produce establish conditions at the kinetic microscales, and the physically significant process—reconnection, heating, particle acceleration, etc., follows as a response. It seems clear that

¹Here we distinguish backscatter from inverse cascade, the latter being back transfer, or upscale transfer, driven by an additional ideal conservation law.

an LES model that would include these effects must be more elaborate than one that focuses mainly on energy flux.

Pursuing a better understanding of the small-scale dynamics in MHD turbulence in the inertial range, and even smaller scale kinetic plasma dynamics in a turbulent medium, has become a very active area of research in recent years. This effort has been boosted by availability of high resolution 3D MHD codes and kinetic plasma codes (fully kinetic, hybrid, and gyrokinetics), as well as a wealth of new observational data regarding solar wind fluctuations down to the electron gyroradius scale (Alexandrova et al. 2009; Sahraoui et al. 2009). These studies have improved our theoretical understanding of the nature of the turbulence cascade and its effects as it progresses from magnetofluid scales, to proton and electron kinetic scales. The continuation of these advances is expected in the next few years to provide a much improved basis for development of SGS models that will enable a new generation of MHD and plasma LES models. In the following, we shall attempt to provide a brief overview of the current state-of-the-art as well as a discussion of key open questions regarding small scale dynamics.

3.1 Do the Small Scales Matter?

Before taking a detailed look at the small-scale dynamics that must be present in any turbulent MHD flow, we must first address a pressing question; do any of these details matter? Recall the central premise of LES introduced in Sect. 1; Since the large scales generally dominate the turbulent transport and energy budget, these are the scales we are most interested in; why should we care about the small scales at all?

There are two answers to this question. First, the small scale dynamics may influence the large-scale dynamics, often in ways we do not yet understand. A notable example is global MHD simulations of magnetic cycles in convective dynamos. Though remarkable progress has been made in recent years, such simulations are still quite sensitive to the nature of the SGS dissipation and the spatial resolution Charbonneau (2015). This is perhaps not a surprise, since the large-scale fields are intimately linked to the small-scale fields by, among other things, the topological constraints associated with magnetic helicity. Large-scale dynamos rely on these linkages to generate magnetic energy and may thus be particularly sensitive to SGS processes.

More generally, the magnetic connectivity has the distinction of depending on microscopic properties such as reconnection activity, while clearly also having an influence on the large scale features of the problem at hand. We now turn to the solar wind as another example that demonstrates this. During solar minimum conditions the fast solar wind is believed to emanate from polar coronal holes while slow wind emerges from nearby regions outside the coronal holes, and perhaps from reconnection activity in coronal streamers. Stated this way it is possible that the boundary between fast and slow wind would be sharp, but this is not observed; instead the transition is more gradual (Rappazzo et al. 2012). It has been suggested that this boundary is thickened by random component interchange reconnection (Lazarian et al. 2012b; Rappazzo et al. 2012) that causes there to be a band of field lines near the boundary that have a finite probability of connecting across this boundary due to dynamical activity. While high resolution codes can simulate small regions near the boundary to demonstrate this phenomenon, in an LES scenario it is doubtful that resolved scales would contain sufficient information to characterize this process. The resolved field lines would be nominal field lines, and if laminar, might maintain a sharp boundary at the coronal hole edges. It would be a challenge for a refined LES/SGS model to incorporate sufficient information about the space-time structure of the unresolved fluctuations so that a model

could be developed to represent both spatial randomization, due to field line random walk, and temporal randomization, due to potentially numerous unresolved reconnection sites.

It is not difficult to find other astrophysical plasma problems that depend on small scale, or even kinetic scale processes, while also having a significant impact on large-scale features. Examples include small and large-scale dynamos (Sect. 5.3) as well as the relative level of electron, proton and minor ion heating in the solar wind or in black hole accretion disks. Here, the small-scale physics plays a critical role in determining the overall magnetic topology, radiative signatures, and thermodynamics of the system, with significant large-scale observable consequences.

The second answer to the question of “why should we care about the small sales at all?” is that the small-scale dynamics can potentially have observable consequences that are regulated by the large-scale flows and fields. A notable example is particle acceleration in solar flares and interplanetary shocks. Sharp gradients in large-scale fields promote small-scale reconnection that often produces a non-thermal spectrum of high-energy particles. These solar energetic particles (SEPs) are an important component of space weather, with potential socio-economic consequences. The small-scale reconnection that produces SEPs also dissipates energy (and other global quantities) and reshapes the magnetic topology. Thus, it may be necessary in some situations to take particle acceleration into account when devising high-fidelity SGS models. In such cases an energy equation formalism would be desirable in order to compute particle diffusion coefficients.

Yet, there are many HD and MHD applications when a simple dissipative SGS model will suffice. Here the large-scale dynamics is insensitive to the small-scale dynamics, provided that the Reynolds and magnetic Reynolds numbers are high enough to resolve coherent structures and capture self-similar cascades. A notable example here is solar granulation (see Sect. 5.1). In this case, one would be satisfied with relatively simple LES models, such as ILES (see Sect. 4).

In order to assess whether or not a sophisticated SGS model is needed, and in order to devise such a model when necessary, one must have a comprehensive understanding of the fundamental physical processes that operate at small scales, and how they influence large-scale dynamics. This is where we now turn.

3.2 Physics of the Small-Scale Cascade

Laboratory plasmas provided the first quantitative indication that MHD turbulence is anisotropic relative to the large scale magnetic field direction (Robinson and Rusbridge 1971; Zweben et al. 1979), generating spectral or correlation anisotropy with stronger gradients transverse to the magnetic field and weaker parallel gradients. Simulations in both 2D and 3D demonstrated the dynamical basis for this effect: propagation of fluctuations along the magnetic field interferes with parallel spectral transfer, while perpendicular transfer remains unaffected (Shebalin et al. 1983; Oughton et al. 1994). Correlation anisotropy of the same type was found to operate relative to the *local* magnetic field (Cho and Vishniac 2000; Milano et al. 2001).

Spectral anisotropy generates a distribution of excitation in wave vector such that average perpendicular wavenumbers are greater than average parallel wavevectors, i.e., $\bar{k}_\perp > \bar{k}_\parallel$, relative to the global field. The degree of anisotropy becomes greater at smaller scales, so, for example the anisotropy of $\nabla \times \mathbf{B}$ exceeds that of \mathbf{B} (Shebalin et al. 1983). Moreover, local correlation anisotropy measured by conditional structure functions (Cho and Vishniac 2000; Milano et al. 2001) is greater than global anisotropy.

Another familiar type of anisotropy that emerges in plasma turbulence at MHD scales is polarization (or variance) anisotropy. In this case one finds that mean square value of

each component of the fluctuations perpendicular to the mean magnetic field is larger than the mean square parallel component. This condition emerges naturally in Reduced MHD treatments of tokamak plasma devices, in which the aspect ratio of the device plays a key role (Kadomtsev and Pogutse 1974; Strauss 1976) and the resulting nonlinear dynamics is both transverse and incompressible, and also requires spectral anisotropy with $k_{\perp} \gg k_{\parallel}$ as discussed above. Later it was shown that Reduced MHD (RMHD) and its transverse fluctuations may be derived by elimination of fast magnetosonic and Alfvénic timescales in solutions of the full 3D compressible MHD equations with a strong mean magnetic field (Montgomery 1982; Zank and Matthaeus 1992).

It is noteworthy that the properties of low frequency, high- k_{\perp} , incompressible fluctuations with transverse polarization, equates in wave vocabulary to dominance of the oblique Alfvén mode, and suppression of the magnetoacoustic modes. This characterization of fully developed incompressible inertial range MHD turbulence—consisting primarily of a highly oblique spectrum of transverse fluctuations has provided a basis for models of plasma turbulence by a number of authors (Montgomery and Turner 1981; Higdon 1984; Goldreich and Sridhar 1995).

While there are a number of differences in these formulations, they have in common that MHD turbulence gets more and more anisotropic at smaller scales. One approach (Goldreich and Sridhar 1995) introduced the term “critical balance,” to describe the fate of weakly interacting Alfvén waves that produce perpendicular spectral transfer until nonlinear (perpendicular) eddy and linear (parallel) Alfvénic timescales become equal. This establishes a relationship between perpendicular and parallel wave numbers that is characterized by $k_{\parallel} \propto k_{\perp}^{2/3}$. As a consequence, one finds $k_{\parallel} \ll k_{\perp}$ at small scales. The same relationship is found in the earlier turbulence theory (Higdon 1984) based on quasi-two dimensional or RMHD spectral transfer (Montgomery 1982; Shebalin et al. 1983) except that the RMHD turbulence energy is mainly confined to the region of wave vector space in which the nonlinear time scale is less than the linear wave timescales. The relationship $k_{\parallel} \propto k_{\perp}^{2/3}$, is common to both, if the wavenumbers are regarded as averages of the energy spectrum in the inertial range. In any case the preference for perpendicular spectral transfer (Shebalin et al. 1983) appears to be a robust result in MHD turbulence and should be considered in SGS modeling when there is a uniform magnetic field or a very large scale magnetic field present.

In addition to the energy spectrum, the inertial range in MHD turbulence is characterized by additional correlations. The velocity and magnetic fields are typically correlated in direction with the sense of correlation coherent within patch-like regions of real space (Milano et al. 2001; Matthaeus et al. 2008a). A complementary idea is that the alignment increases systematically with decreasing scale (Boldyrev 2006; Mason et al. 2006). It is also documented that turbulence produces patchy, localized correlation of other kinds in MHD (Servidio et al. 2008), and at least some of these appear to be related to the tendency for turbulent relaxation (Ting et al. 1986; Stribling and Matthaeus 1991) to proceed locally in cellular regions, such as flux tubes, as a faster, intermediate step towards global decay and relaxation. The types of correlations produced locally and rapidly in this way include (but are not limited to), not only the Alfvénic correlation (velocity and magnetic field), but also the Beltrami correlation (velocity and vorticity) and the force free correlation (magnetic field and electric current density). All lead to depression of nonlinearity in the inertial range of scales, as seen in the emergence of Beltrami correlation in HD (Pelz et al. 1985).

It is not entirely clear how or whether these additional correlations should be included in LES/SGS modeling of the smaller scale MHD cascade. On the one hand, the diversity in possible long-term relaxed states suggests dominance of different relaxation processes for different parameter regimes. For example, to achieve global dynamic alignment, any

excess mechanical or magnetic energy would need to be dissipated. Similarly, in order to achieve global selective decay of energy with constant helicity (Montgomery et al. 1978; Matthaeus and Montgomery 1980), also known as Taylor relaxation (Taylor 1974), would require that mechanical energy be entirely dissipated while magnetic energy remains. Presumably these alternative decay prescriptions place different requirements on the nature of dissipation models. Dynamo action with injected mechanical helicity at intermediate scales also places requirements on transfer and dissipation rates of energy, magnetic helicity and kinetic helicity (e.g. Brandenburg 2001; Brandenburg and Nordlund 2011; Brandenburg and Subramanian 2005). On the other hand if the processes being modeled are principally dependent on the decay rate of energy, it may be possible to define energy fluxes with relatively simpler prescriptions, such as by partitioning transfer between direct and inverse cascade rates. How these issues will influence improved and accurate LES/SGS models for MHD in the future is a current research-level problem that is intimately tied in with prospects for universality in MHD turbulence, or perhaps universality within classes of MHD behavior.

While it will likely be necessary to learn more about MHD and kinetic scale cascades to build more complete models, it is noteworthy that considerable theoretical progress has been made, including computations, by assembling turbulence models that may lie somewhat outside of a strictly-defined LES concept. These models typically have concentrated on selected effects that are thought to be dominant for the chosen problem. Examples of such models are mean field electrodynamics (Moffatt 1978; Krause and Rädler 1980) often used in dynamo theory, Reynolds averaged MHD models such as those used for solar wind modeling (Usmanov et al. 2014) and hybrid models based on multiple scale analysis and Reynolds averaging (Yokoi et al. 2008). In any of these models, we should note that a turbulent resistivity would have essentially the same effect as an “anomalous” resistivity, by which we mean a contribution to resistivity due to small scale (and also unresolved) kinetic plasma effects. This is also an area that has been well studied (e.g. Biskamp 2000).

As an example of a non-traditional LES approach, Yokoi et al. (2013) describe a novel self-consistent mean-field theoretical model of turbulent MHD reconnection, highlighting cross-helicity dynamo effects. In this, essentially sub-grid, model the effects of small-scale turbulence are represented by two additional terms in the Ohm’s law: one proportional to the turbulent energy density and describing standard effective turbulent resistivity, and the other, new term, proportional to turbulent cross-helicity $W = \langle \mathbf{u}' \cdot \mathbf{b}' \rangle$ and the large-scale vorticity $\boldsymbol{\Omega} = \nabla \times \mathbf{U}$. Though this model appears to capture the influence of small-scale turbulence on large-scale reconnection (Yokoi et al. 2013), Grete et al. (2015) found that it does not perform well for supersonic MHD turbulence, where it fails to reproduce the turbulent electromotive force (EMF) obtained from high-resolution ILES (standard eddy diffusion models also fail in a similar way). More work is needed to determine its viability in different circumstances. Indeed, this applies to all SGS models; to the extent that it is feasible, their validity and scope should be evaluated by comparing them to high-resolution DNS/ILES (e.g. Grete et al. 2015; Meheut et al. 2015) and/or to kinetic plasma simulations.

Having introduced some prominent features of the physics of MHD turbulence at small scales, we will now focus on some recent findings from respective studies that are relevant to the fate of the MHD cascade at smaller scales. A central issue for many applications in space and astrophysics is how the cascaded energy is actually dissipated, and in some astrophysical systems, eventually radiated away. For the present purposes the notion of dissipation may be described as the irreversible conversion of large scale or fluid scale energy into microscopic kinetic degrees of freedom. Important questions that have been recently addressed in this area include the response of test particles to MHD electromagnetic fields, kinetic effects including dissipation of cascaded MHD fluctuations and the response in the

form of heating, and the role of magnetic reconnection, current sheets and tearing, and the associated macroscopic effects of changes in magnetic topology and connectivity.

3.3 Energization and Transport of Test Particles

The most primitive model of kinetic response to MHD-scale fields is given by the test-particle approximation in which the trajectory of individual plasma particles is assumed to be determined by the Newton-Lorentz force law, neglecting all feedback of the particle motion on the rest of the plasma or on the electromagnetic fields. The basic physics of acceleration, scattering and transport, especially of suprathermal and energetic particle populations, is often discussed in a first approximation using a test particle approach (e.g. Bell 1978; Jokipii 1966). Not only are test particle studies useful in understanding energy dissipation, but in some cases, e.g., cosmic rays and solar energetic particles, it is the response of the test particles to the large scale fields, and the subgrid scale fields, that is the essential output of the research.

A self-consistent model extending beyond test particles is needed for accurate representation of the effects on dissipation of slower populations of plasma particles, say, those moving at a few Alfvén speeds or less. Nevertheless, in spite of its shortcomings, the test particle approach, implemented in concert with MHD computations, has been valuable for investigation of potential mechanisms of energization and dissipation prior to emergence of computational capacities that enable equivalent self-consistent kinetic modeling.

A good example of this is the use of test particles in the elucidation of the role of reconnection and turbulence in energization of suprathermal particles. Spectral methods, having favorable resolution properties for turbulence, were able to describe the interplay of test particle energization and nonlinear reconnection at a relatively early stage (Ambrosiano et al. 1988). In the presence of strong fluctuations, reconnection does not settle in to smooth solutions anticipated from tearing mode theory, and instead remains unsteady and bursty, and when the Reynolds number at the scale of the dominant current sheets exceeds a few hundred, the fluctuations lead to multiple small magnetic flux structures, or secondary islands (Matthaeus and Lamkin 1985, 1986; Biskamp 1986). This subject is revisited in more detail below in Sect. 3.5.

Here we note simply that such structures can entrain or temporarily trap test particles, and are strongly associated with the most efficiently energized particles. This entrainment and energization was found to occur between magnetic X-points and O-points, as was later found in much greater detail and realism using high resolution kinetic plasma codes (e.g. Drake et al. 2006).

It is clear that even a simple model employing MHD simulation fields and test particles can begin to identify kinetic effects beyond simple energization. Studies showed that small gyroradius particles (e.g., electrons) tend to be accelerated in the direction along the electric current sheets, that is, parallel acceleration, while heavier particles (protons, etc) are energized in their perpendicular velocities (Dmitruk et al. 2004). Self-consistent kinetic simulations also were able to find this effect, and in fact it is now understood through plasma simulation that the regions *in and near* current sheets are sites of enhanced kinetic effects such as suprathermal particles, temperature anisotropies, large heat flux, and in general non-Gaussian features of the proton distribution function (e.g. Servidio et al. 2012; Karimabadi et al. 2013).

More recent test particle studies that employ weakly 3D RMHD simulations (Dalena et al. 2014) suggest that energization of a single species of test particle progresses through at least two stages in the presence of a strong guide field with nearly two dimensional low

frequency fluctuations: First, at lower energies the particles are energized in their parallel velocities, and mainly while entrained near reconnection sites inside of current sheets and in essentially in accord with the classical neutral point acceleration mechanism. This is also sometimes called “direct acceleration.” As suprathermal energy grows and the gyroradii become larger than the typical thickness of the current sheets, the energization of test particles continue, but with enhancement of perpendicular velocities. This has been described as a “betatron” process associated with an inhomogeneous perpendicular electric field found near to, but outside of strong reconnection sites (Dalena et al. 2014). This test particle result provides more detail on earlier results on acceleration in turbulence (Dmitruk et al. 2004; Chandran 2010).

The marriage of test particle studies with high resolution MHD simulation has led to a number of insights and questions that are of relevance to ongoing efforts to develop SGS models for MHD and plasmas. For example:

- When are the processes of cascade, reconnection, test particle energization, and dissipation, related? While it is fairly clear that a broad-band cascade requires reconnection to occur at various scales along the way, the fact that test particles respond to the associated inhomogeneities suggests that dissipative processes may be intertwined in this process.
- The topology of the magnetic field becomes fuzzy when there are numerous small secondary islands, so trapping, reconnection, coalescence and particle energization will in general not be explicitly resolved in an SGS/LES scheme for a large system. Most likely these features will need to be understood well enough to develop a statistical or phenomenological model.
- If tracking test particle populations at a statistical transport level remains a scientific priority in an LES context, then a requirement will be to follow parameters needed for SGS transport models, such as SGS energy, characteristic length scales, and possibly spectral features such as anisotropies, e.g., to capture possible resonances.

3.4 Kinetic Effects, Dissipation Processes and Heating

Once cascading fluctuations reach scales at which kinetic effects become important, MHD is no longer applicable. In practical terms, this means that for an ion-electron plasma, when the cascade arrives at scales as small as either the ion gyroradius scale, ρ_i , or the ion inertial scale $d_i = V_A/\Omega_{cp}$, kinetic effects become important and even dominant. For wavenumber k the corresponding kinetic range is indicated by $k\rho_i \geq 1$ or $kd_i \geq 1$. To retain effects like finite Larmor radii and Landau damping in this regime, one has to employ a kinetic description.² Since in space physics and astrophysics we are often dealing with low density plasmas for which the collisionality is very weak, it is important to keep in mind that some type of effective “collisions” will inevitably cause departures from an idealized model such as the Vlasov-Maxwell equations. Fundamental effects such as an increase of system entropy and relaxation towards thermal equilibrium, will rely on the presence of these formally small contributions to the kinetic equations (Klimontovich 1997; Schekochihin et al. 2009). In any case, given the enormous computational cost of nonlinear kinetic simulations in six phase-space dimensions, such studies often fall into the category of “extreme computing.” Results on turbulence energy dissipation and relaxation in turbulent plasmas, employing particle-in-cell (PIC) Vlasov code and Eulerian Vlasov codes, are just starting to appear

²By kinetic description we mean a dynamical description of the plasma that involves only the one-particle distribution function which depends on velocity, position, and time.

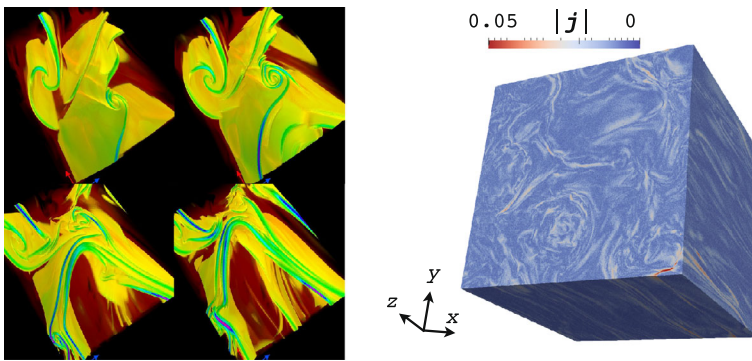


Fig. 3 (Left) Volume rendering of magnitude of current density J in the same small region of a high resolution 3D MHD simulation at four different times, showing complex spatial structure and evolution in time (adapted from Mininni et al. 2008). (Right) Volume rendering of J from a 2048^3 PIC simulation of plasma turbulence, in a periodic box of side 83.8 thermal proton gyroradii. Again, fine scale structure is evident, now at kinetic scales (Courtesy of V. Roytershteyn, to be published.)

in the literature (e.g. Daughton et al. 2011a; Servidio et al. 2012; Karimabadi et al. 2013; Haynes et al. 2014).

In light of the impressive continued growth of supercomputing power as we head towards the exascale era, it may be expected that kinetic simulations will be at the forefront of research into the fate of cascaded energy at kinetic scales in the years to come. Meanwhile, various reduced models are being used to complement fully kinetic studies. These include hybrid (fluid electrons and kinetic ions), gyrokinetic and gyrofluid models, and an array of fluid models that contain some kinetic effects (Hall MHD, multifluid, Finite Larmor radius MHD, etc.)

Fully kinetic 3D PIC simulations of turbulence and reconnection have recently revealed interesting details about kinetic response to cascading MHD scale fluctuations. In 3D, ion-scale current sheets spontaneously develop turbulence through various instabilities, producing a chaotic 3D magnetic field structure (Daughton et al. 2011a). Examples of fine scale current structures in high-resolution MHD and kinetic simulations are shown in Fig. 3. Interestingly, however, both the reconnection rate and the mechanism for breaking the frozen-flux law seem to be unaffected, being close to those obtained in 2D simulations. Numerical experiments with different types of initialization, such as velocity-shear-driven kinetic turbulence (Karimabadi et al. 2013) show that current sheets and intermittency can form in both 2.5D PIC simulations as well as 3D PIC simulations. Furthermore, kinetic activity of various types, including heating, appears to be concentrated near sheet-like current structures (see also Servidio et al. 2012; Wan et al. 2012a), which lends credence to the emerging idea that a large fraction of kinetic heating may occur in or near current sheets and related structures. (For the MHD analogue of intermittency associated with current sheets, see Sect. 3.4.) Some wave activity is also identifiable in the above examples, although in terms of the partitioning of energy, this seems to be the exception rather the rule when broad-band turbulence develops at kinetic scales (Parashar et al. 2010; Verscharen et al. 2012; Karimabadi et al. 2013). Kinetic scale complexity and intermittency is also observed using recent high resolution observations in the solar wind (Perri et al. 2012; Wu et al. 2013a).

Even with recognition of this complexity at kinetic scales, efforts continue to analyze the type of wave mode, or perhaps several types, that might be viewed in some sense as the elementary excitations from which the turbulence is constructed. There are actually several

approaches that may be described as a wave turbulence approach. On the one hand there is the formal weak turbulence theory (e.g. Galtier et al. 2000) that considers the cases in which the leading order dynamics is that of propagating waves that obey, to a first approximation, a dispersion relation that assigns a frequency to each wavevector. Another view is that the distinguishing characteristics of wave modes are the polarizations and wave vector directions, which suffice to establish an identification.

Substantial research has been devoted to models that are built upon the premise of wave modes that couple to produce wave turbulence in the nonlinear regime. One class of such models, defined in the MHD regime, is the Goldreich-Sridhar theory (Goldreich and Sridhar 1995), (also called “critical balance” after one particular assumption that is made in the theory; see Sect. 3.2). This theory assumes that all possible excitations are Alfvén modes, having polarizations strictly perpendicular to the applied mean magnetic field. The usual argument is that other wave modes evolve semi-independently so that the evolution of the Alfvén waves and their mode-mode couplings can be computed independently of the magnetosonic wave turbulence. This idea is also routinely carried over to kinetic regimes, in which it is assumed that distinct wave modes, such as kinetic Alfvén waves (KAW), or whistlers, will evolve independently. Numerical evidence is usually invoked to support this assumption, but the idea remains somewhat controversial. For example, 2.5D kinetic simulations that are initiated with Alfvén modes, i.e., zero parallel variance, appear to generate parallel variance fairly rapidly, although at a lower level. Thus, in wave terminology, magnetosonic mode turbulence is generated by Alfvén mode turbulence within the time span of the current generation of simulations which are relative short due to finite computational resources, typically less than, say, 1000 proton cyclotron periods. Furthermore it is well known that the parallel variance component of solar wind turbulence is small but nonzero, as in the famous “5:4:1” observations by Belcher and Davis (1971) using Mariner data.

Goldreich-Sridhar turbulence, which is purely Alfvén mode, evolves from a wave state through standard weak turbulence couplings towards the critical balance state, provided that the zero frequency modes (purely 2D nonpropagating fluctuations) are absent or very nearly absent. This results in a wave turbulence that is highly oblique, with mainly near-perpendicular wave vectors involved in the dynamics. At small scales approaching the kinetic range, the oblique Alfvén modes in Goldreich-Sridhar theory naturally go over to Kinetic Alfvén waves (Hollweg 1999), which have received substantial attention recently in solar wind observations (Bale et al. 2005; Sahraoui et al. 2010)

Another wave mode discussed in connection with wave turbulence and a possible role in the kinetic range of solar wind dynamics is the whistler mode (Hughes et al. 2014), which generally is at higher frequencies than the KAWs and probably has lower amplitude in the solar wind, but may still play a role in the operative dissipation mechanisms.

Much of the debate concerning relative roles of wave modes has taken place in the context of recent high resolution measurements of fluctuations in the dissipation range of solar wind turbulence (Bale et al. 2005; Alexandrova et al. 2009; Sahraoui et al. 2009, 2010). First, it was observed that the electric and magnetic field fluctuations as well as the density fluctuations in the scale range of $\rho_i^{-1} \ll k_{\perp} \ll \rho_e^{-1}$ display power law (not exponential) spectra. While the knee at $k_{\perp} \rho_i \sim 1$ was originally attributed to some form of damping, e.g., proton cyclotron damping or Landau damping of kinetic Alfvén waves (KAWs), it was later suggested that the observed power law exponents can be explained solely on the basis of dispersion effects at these scales (Stawicki et al. 2001). Consequently, this scale range is now sometimes also called a “dispersion range”. Neglecting cyclotron absorption at the proton resonance, it may be that significant ion/electron dissipation sets in, respectively, at sub-ion scales, $k_{\perp} \rho_i \gg 1$, and electron scales, $k_{\perp} \rho_e \sim 1$. Beyond the electron scales one

might expect the occurrence of exponential spectra (Alexandrova et al. 2009) although there are also observations consistent with yet another power law (Sahraoui et al. 2009). Clearly, the physics of this entire sub-ion scale range is of interest to understanding the heating of turbulent space and astrophysical plasmas. The relative importance of ion and proton kinetic mechanisms that might give rise to dissipation is likely determined by turbulence amplitude (Wu et al. 2013b) in addition to kinetic plasma parameters such as the ion-to-electron temperature ratio τ and the plasma beta β .

Standard approaches to studying the physics of the kinetic range of turbulence are Lagrangian PIC and Eulerian solutions of the Vlasov equation, as well as the hybrid (fluid electron) variants of each of these. However, there have been special reduced models that have emerged that include interesting subsets of the relevant physics. Nonlinear gyrokinetic theory (see Schekochihin et al. 2009, and references therein) has been developed in the context of magnetic confinement fusion research since the early 1980s, and today it serves as the workhorse for computations in tokamak research. An adaptation of gyrokinetics, as embodied e.g. in the GENE (Jenko et al. 2000) and AstroGK (Howes et al. 2008) codes, includes a subset of possible gyrokinetic effects, and has been proposed as a model for turbulence investigations in weakly collisional, strongly magnetized space and astrophysical plasmas from the inertial range through the ion and electron kinetic ranges. The main limitation of standard gyrokinetic theory is that it is based on a low-frequency (compared to the particles' cyclotron motion) ordering, assuming a decoupling the fast gyrophase dependence from the slow gyrocenter dynamics. Notably, this version of gyrokinetics lacks cyclotron resonance and therefore maintains particle magnetic moments, thus placing it at odds with some theories of solar wind and coronal heating. We note in passing that this constraint can be removed if necessary, leading to extended versions of gyrokinetics (Qin et al. 2000). In any case, the formulation does include the physics of kinetic Alfvén waves, and goes over to Reduced MHD in appropriate limits. As such gyrokinetics is well suited to describe the Goldreich-Sridhar cascade. Gyrokinetics provides a computationally efficient method to study certain problems, and it has been argued that it does capture the physics needed to describe the observed turbulence (Howes et al. 2008) and heating (TenBarge et al. 2013); this however remains a topic of lively discussion. It is also worth noting that gyrokinetics itself has been treated using an LES approach (Morel et al. 2011, 2012).

Gyrofluid theory is an attempt to reduce gyrokinetics to a multi-fluid approach via calculating moments and closing the resulting hierarchy of equations by providing suitable closure schemes (Hammett and Perkins 1990; Passot et al. 2012). Kinetic effects like finite Larmor radii and linear Landau damping can be retained with reasonable accuracy, provided that the closures are carefully constructed. Also pioneered in the context of magnetic confinement fusion research in the 1990s, gyrofluid models have more recently been tailored and applied to various space and astrophysical problems. The development and refinement of this approach is a subject of on-going research.

It is at present unclear which model or models will provide what is needed for development of effective LES for low collisionality plasmas. If we knew which processes were important, then selection of the appropriate reduced description models such as 2.5D kinetic codes, hybrid codes with fluid electrons, gyrokinetic codes or gyrofluid codes, may provide the efficiency needed to arrive at the needed answers more quickly. However if those processes need to be identified, then more demanding 3D fully kinetic Vlasov or PIC representations may be required.

We close the section with a few remarks concerning the prediction of turbulence spectra in the kinetic range and the associated ambiguities of identifying dissipation mechanisms. Within a wave turbulence framework, one may establish a contrast between expectations of

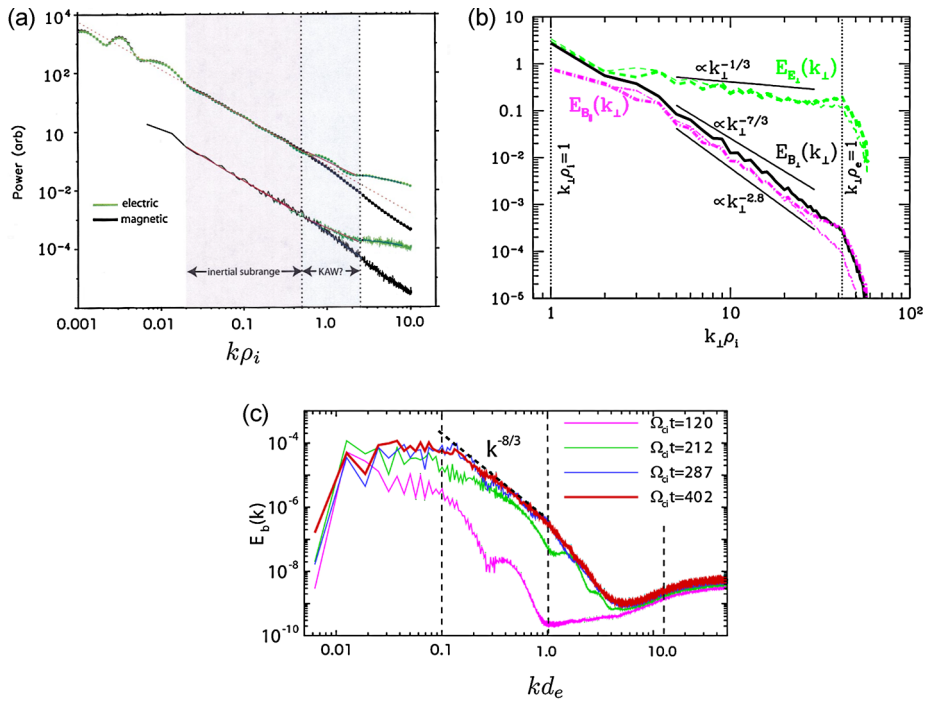


Fig. 4 (a) Magnetic and electric field spectra in the solar wind obtained from in situ measurements by the Cluster spacecraft, from Bale et al. (2005). Corresponding spectra from (b) gyrokinetic simulations (Howes et al. 2008), and from (c) electromagnetic PIC simulations (Karimabadi et al. 2013) are also shown for comparison. In frames (a) and (b), wavenumbers are normalized by the thermal ion gyroradius ρ_i ; in frame (c) the wavenumbers are normalized by the electron inertial scale $d_e = c/\omega_{pe} = V_A/\Omega_{ce}$

KAW-mode turbulence and whistler-mode turbulence. Solar wind observations indicate a dispersive effect near the ion inertial scale that has been associated with KAWs (Bale et al. 2005) and with gyrokinetics (Howes et al. 2008); see Fig. 4. However this can qualitatively be explained by any dispersive processes that include a Hall effect (Matthaeus et al. 2008b), so this is not a conclusive observation. On the other hand, the KAW and whistler dispersion relations, examined in detail in the observations, seem to favor KAWs more than whistlers in kinetic wave number ranges above $k\rho_i \sim 1$ (Sahraoui et al. 2009). However a strong conclusion cannot be derived from this concerning dissipation processes because, first, we do not know that the dissipation occurs at these wavenumbers—if it were to occur at much higher electron wavenumbers, there may be whistlers or other higher frequency waves that actually do the dissipating; and second, we do not know for certain that a wave turbulence treatment is even appropriate. Figure 4 compares solar wind observations with both gyrokinetic and kinetic simulations. In all cases the magnetic spectra break to something steeper than the inertial ($-5/3$) range at or near ion kinetic scales. The latter may be the thermal ion gyroradius ρ_i or, especially at low plasma beta, the ion inertial scale $d_i = c/\omega_{pi} = V_A/\Omega_{ci}$. (Note that, when the plasma β is unity, $\rho_i = d_i$.) The PIC result shows a similar spectrum (possibly closer in slope to $-8/3$ than to $-7/3$) with wavenumber normalized by electron inertial scale $d_e = c/\omega_{pe}$. Note that $d_e/d_i = \sqrt{m_e/m_i}$. Evidently the spectra themselves do not strongly differentiate between models. Additional examples from computations are shown in Matthaeus et al. (2008a), Sahraoui et al. (2009), and Alexandrova et al. (2009).

If stochastic acceleration and scattering of orbits (Dmitruk et al. 2004; Chandran 2010; Dalena et al. 2014) in or near current sheets absorbs substantial fluctuation energy, then one may have to look beyond linear damping of wave modes for an effective dissipation mechanism. Other heating processes are also evidently available near turbulent reconnection sites and other coherent structures that are seen in very high resolution kinetic simulations (Karimabadi et al. 2013; Wan et al. 2012b). Furthermore, other kinetic instabilities (such as firehose and mirror instabilities) and the fluctuations they produce may be particularly active near coherent structures (Servidio et al. 2014) and sharp gradients (Markovskii et al. 2006), and these may contribute to dissipation. More work will have to be done to investigate, confirm and refine any of these emerging scenarios, in particular with respect to the role of non-Maxwellian velocity space features seen in fully kinetic nonlinear simulations (Hellinger and Trávníček 2013; Servidio et al. 2012, 2014).

3.5 Magnetic Reconnection, Current Sheets and Intermittency

Magnetic reconnection is an important element of the dynamics of plasmas, and has been widely studied for more than half a century both theoretically and in applications. The basic theory has been well reviewed in terms of MHD theory (Biskamp 2000; Forbes and Priest 2000; Zweibel and Yamada 2009), the complications that emerge in three dimensions (Priest and Schrijver 1999), the transition from MHD to kinetic behavior (Birn and Priest 2007), and in situ spacecraft observations (Birn and Priest 2007), and plasma experiments where kinetic effects begin to become important (Yamada et al. 2010). We will not attempt to reproduce such reviews here. Many of the computational models in which reconnection has been studied (see references above) have been formulated to include kinetic effects, but in small domains with simple boundary conditions and smooth initial data, often based upon an equilibrium current configuration. In such cases the reconnection that is studied may be viewed as *spontaneous reconnection*, which itself is a rich and well-studied approach. However it has become increasingly clear that the traditional way of studying magnetic reconnection via standard equilibrium current-sheet setups needs to be complemented by investigations of reconnection in more complex environments, and in particular in self-consistent turbulent environments. As of now, we are still in the early stages of understanding this more complex situation, in particular with respect to kinetic treatments of quasi-collisionless systems. One key question in this context is the degree to which phenomena associated with reconnection, such as particle acceleration, can act as an alternative route to dissipation. Here we can provide only a brief overview of this active research topic, which has been examined from a variety of similar approaches.

The first description of turbulent reconnection (Matthaeus and Lamkin 1986), an initial value problem consisting of a sheet pinch evolving in the presence of a specified broad-band spectrum of fluctuations, might properly be called “reconnection in the presence of turbulence.” In this case one finds bursty, nonsteady reconnection, in which one observes sporadically forming intense current sheets and vortex quadrupoles, as well as transient multiple X-points. This approach was found to lead to elevated rates of reconnection, for resistive MHD, the increase for large systems being comparable to or greater than the increase due to Hall effect (Smith et al. 2004). An important dynamical feature of this problem is the *amplification* of the turbulence due to nonlinear instability of the initial configuration and subsequent feedback (Lapenta 2008).

Another approach, which has usually been applied in three dimensions, also begins with a sheet pinch initial condition, but instead of supplying turbulence through an initial spectrum of fluctuations, a random source of fluctuations acts continuously through a forcing function

applied to the region surrounding and including the current sheet (see Kowal et al. 2009; Loureiro et al. 2009; Lazarian et al. 2012a, and references therein). This too gives rise to strong turbulence effects, and as might be expected, the reconnection rate generally is tied closely to the imposed turbulence amplitude.

Still another approach in understanding the relationship between turbulence and reconnection is to initialize a system with a large number of magnetic flux tubes, as well as random velocity fields, such that the initial state triggers a complex cascade. The turbulent dynamics leads to interactions between various pairs of adjoining magnetic flux tubes (or magnetic islands), leading to reconnection with widely distributed reconnection rates, studied in 2D MHD (Servidio et al. 2009, 2010) and more recently in Reduced MHD (see below and Wan et al. 2014). This type of “reconnection in turbulence” might be viewed as similar to both problems described above, but with the random perturbations caused by the cascade itself, rather than being imposed by an initial spectrum or by a prescribed forcing function. Some have argued that for systems having many flux tubes, this might be viewed as a more natural way to drive reconnection with turbulence, but it has the disadvantage of requiring a large system, both to establish a high Reynolds number cascade, and to adequately resolve the smaller scale current sheets.

A further complication in understanding reconnection is that its geometry can become quite complex in three dimensions (Priest and Schrijver 1999), departing strongly from the familiar two dimensional forms. Nevertheless it seems rather certain that in 3D models, as in 2D models, coherent electric current structures, including sometimes complex sheet-like structures (Mininni et al. 2008), continue to play an important role. For example, current sheets in RMHD models occupy a central role in models of coronal heating that have been studied (Einaudi and Velli 1999; Dmitruk et al. 1998; Rappazzo et al. 2010) in the so-called nanoflare scenario. This model is typically viewed as an implementation of the Parker problem (Parker 1972) in which coronal field lines are stirred from below by photospheric motions, which causes a braiding or tangling of flux tubes, the formation of current sheets between pairs of them, and subsequent bursty reconnection and heating. Recently there has been further progress in understanding the local statistics of current sheet dynamics in the weakly three dimensional Reduced MHD model discussed above, thus advancing out understanding of the role of these current sheets in reconnection, heating and intermittent dissipation in 3D. Other, simpler, models can be constructed that take into account the phenomenology of MHD by stipulating that dissipative structures are current and vorticity sheets and that the typical time of energy transfer to small scales is modified in MHD when taking into account the role of Alfvén waves (see, e.g. Grauer et al. 1994; Politano and Pouquet 1995).

Zhdankin et al. (2013) carried out a quantitative statistical analysis of current sheets that emerge in RMHD turbulence, and reported on the distribution functions of current sheets with respect to their dimensions, peak current densities, energy dissipation rates and other characteristics. Wan et al. (2014) reported a similar study using an RMHD coronal heating model, confirming many of the results in Zhdankin et al. (2013), while also computing the distribution of reconnection rates and demonstrating the statistical connection between current sheet dimensions and characteristic turbulence length scales. An interesting result obtained in both the above studies is that the locus of maximum dissipation rate, always the peak of current density for scalar resistivity, is *not* always, or even usually, located at the component X-points. This is a property also found in laminar asymmetric reconnection (Cassak and Shay 2007), having different magnetic field strength on the two flow sides of the reconnection zone. Perhaps not surprisingly, larger reconnection rates are well correlated with the proximity of the current maximum to the X-type critical point. These purely spatial

analyses were extended into the temporal domain by Zhdankin et al. (2015) who tracked the evolution of dissipative structures over time and measured the statistics of their lifetimes and total energy dissipation. The results obtained so far for reconnection in RMHD are clearly valuable in providing some information about the 3D case, and are specifically applicable to low plasma beta, highly anisotropic systems driven at low frequencies, such as the coronal flux tube problem. However the general 3D case will undoubtedly contain significantly greater complexity (see e.g. Mininni et al. 2008), much of which remains to be explored.

The dynamics of the formation of current sheets and other small scale coherent structures is of great importance in understanding the intermittent cascade and its fate. Furthermore, current sheet formation may be quite different in a large turbulent system than it is in a laboratory device in which the magnetic field to leading order is large scale, laminar, and controlled by external coils. For example, it is well known that ideal-MHD flows that develop in turbulence give rise to intense thin current-sheet structures (Frisch et al. 1983; Wan et al. 2013). The ideal process of current sheet generation, observed at short times in high resolution MHD simulations (Wan et al. 2013), apparently gives essentially identical higher order magnetic increment statistics as are seen in comparable high Reynolds number simulations—so we can understand that intermittency and the drivers of the conditions that lead to reconnection are ideal processes. In retrospect, this could have been anticipated in Parker's original discussion of coronal flux tube interactions (Parker 1972). Reconnection may subsequently be triggered at these sites, resulting in dissipation of turbulent magnetic field.

The process of current sheet formation in the presence of weak dissipation can also involve multiple magnetic X-points and secondary islands or flux tubes. This was originally observed in reconnection with finite background turbulence, and in that context it was suggested that secondary islands might elevate the reconnection rate (Matthaeus and Lamkin 1985, 1986; Loureiro et al. 2009). Biskamp (1986) suggested that secondary islands might emerge due to a linear instability of thin current sheets above magnetic Reynolds numbers of about 10^4 . More recently this instability was revisited based on the recognition that the tearing instability can become much faster if it originates in a current sheet already thinned to the Sweet-Parker thickness (Loureiro et al. 2007; Bhattacharjee et al. 2009). The occurrence of this "plasmoid instability" has been supported by simulation studies using MHD and PIC codes (Samtaney et al. 2009; Daughton et al. 2011b; Loureiro et al. 2012). Loureiro et al. (2007) found that the growth rate of the secondary tearing instability of a Sweet-Parker reconnection layer is higher than the inverse global Alfvén transit time along the layer. M. Velli and collaborators (e.g. Pucci and Velli 2014) have argued that this result means that, in reality, such a layer cannot be formed in the first place. In fact when the linear growth rate of tearing instability equals the inverse of $\tau_A = L/V_a$ the current sheet necessarily is disrupted. This occurs at $a/L \sim S^{-1/3}$, where S is the global Lundquist number, $S = LV_A/\eta$. In the asymptotic limit $S \rightarrow \infty$, this value is much greater than for the SP layer, which suggests that as a current layer is being formed, it is disrupted by secondary tearing well before it reaches the SP stage. A similar conclusion was presented by (Uzdensky and Loureiro eprint 2014).

As mentioned above, one also finds the occurrence of numerous secondary islands in a turbulence context, and this will also be the fate of any multiple island scenario at finite amplitude. High resolution 2D MHD turbulence simulations display a proliferation of magnetic X-points at sufficiently high magnetic Reynolds number R_m (Wan et al. 2012b), with the number of X-points and flux tubes observed in the simulations, scaling as $R_m^{3/2}$. A cautionary word is that secondary islands (or plasmoids) also form due to numerical error, and there is a requirement for careful resolution studies (Wan et al. 2010) to ensure that complex

multiple plasmoid reconnection is physical and not numerical. It is unclear at present what precise relationship exists between plasmoid instability and generation of secondary islands turbulence. It is noteworthy that simulations, even laminar cases, usually trigger reconnection with a finite amplitude perturbation, and by the time multiple islands are observed there are many finite amplitude modes participating. Whether the origin is instability or cascade, it seems certain that at high magnetic Reynolds numbers, reconnection zones will be complex, even in 2D, so that the details of the many individual reconnection processes will almost certainly not be resolved in LES, but rather their aggregate effect will need to be built into a SGS model.

To close this section we note first the implications of the evolving perspectives on reconnection for an application, say, solar coronal heating. In such a complex driven system that is far from equilibrium, one should properly view current sheet formation, dissipation, magnetic reconnection, and nanoflares, not as independent processes, but rather as outcomes of a nonlinear MHD-turbulent cascade in a self-organized solar corona. Building such effects into an LES/SGS model will be challenging.

Finally for completeness we list some of the outstanding questions that emerge from this discussion:

1. Do singular (ideal) structures matter for the dissipative case?
2. Does the 2D case matter to understand the 3D case?
3. Are rotational discontinuities a central piece of 3D reconnection?
4. Does current sheet roll-up play a role?
5. What role do invariants (magnetic and cross helicity) have in reconnection?
6. Is the rate of dissipation independent of Reynolds number?
7. What are the dissipative and/or reconnecting structures, and how to identify them in a real (natural) system?
8. What is the role of the magnetic Prandtl number?
9. Do small-scale kinetic effects that emerge in reconnection alter large-scale dynamics?
How?
10. Can Adaptive Mesh Refinement help in a general approach?

4 LES in MHD

The discussion in the previous section (Sect. 3) highlights some of the challenges in devising reliable SGS models for LES of MHD turbulence. In this section we describe in more detail the practical implementation of LES/SGS modeling, focusing on explicit approaches that employ formal filtering operations designed to decompose the flow into large and small-scale components. The large-scale motion is computed by solving the filtered non-stationary equations of MHD while the SGS terms are parameterized and expressed in terms of the filtered quantities. Though real plasma flows are likely much more subtle (Sect. 3), current MHD-LES models often assume that the subgrid scales (SGS), also referred to as subfilter-scales (SFS), are relatively isotropic, homogeneous, and universal.

LES is a method for simulation of flows with large Reynolds numbers. It is generally not valid for low Reynolds number flows since it assumes that there is a substantial (order unity) nonlinear transfer to small scales. Furthermore, as discussed in Sect. 3, the usual assumption of isotropy at small scales may not be realized. This may occur in rotating and/or stratified flows if the cut-off wavenumber where the filter is applied is in the anisotropic range. And, it may occur more generally in turbulent MHD flows where anisotropy may progressively

increase toward smaller scales unless this is mitigated by turbulent reconnection processes which may help recover isotropy.

Initially the Large Eddy Simulation technique was developed for the simulation of HD turbulence of neutral fluids, particularly in the context of atmospheric and engineering applications (Meneveau and Katz 2000; Sagaut 2006; Glazunov and Lykossov 2003). This has been extended to MHD turbulence by several authors who adapted known HD closures to the MHD case and developed new SGS models. (Agullo et al. 2001; Müller and Carati 2002a,b; Yoshizawa 1987; Zhou and Vahala 1991; Knaepen and Moin 2003). Our discussion of the general approach follows that given in Chernyshov et al. (2006a). Our intention is to illustrate how the MHD equations can be cast into a traditional LES framework. We make no attempt at a comprehensive survey of existing LES/SGS models. For alternative approaches see Miki and Menon (2008), Grete et al. (2015), and Schmidt (2015). Of particular note is the model presented by Grete et al. (2015) in which the SGS stress tensor involves nonlinear correlations between the resolved (filtered) velocity and magnetic field gradients, along with Smagorinsky-like expressions for the SGS kinetic and magnetic energy proportional to the corresponding rate of strain tensors. This is based on a Taylor expansion of the velocity and magnetic field within a filter box as originally proposed for HD by Woodward et al. (2006a).

As stated above, a LES applies a filtration operation to the primitive equations as suggested by Leonard (1974).³ For the incompressible MHD equations, the filter G satisfies the following normalization property:

$$\int_a^b G(x_j - x'_j, \bar{\Delta}_j) dx'_j = 1. \tag{1}$$

Here $G(x_j - x'_j, \bar{\Delta}_j)$ is the filter itself, of width Δ_j . Then, the filtered velocity is expressed as follows:

$$\bar{u}_j = \int_a^b u(x'_j)G(x_j - x'_j, \bar{\Delta}_j) dx'_j, \tag{2}$$

where $a = x_j - \frac{1}{2}\bar{\Delta}_j$ and $b = x_j + \frac{1}{2}\bar{\Delta}_j$, $\bar{\Delta}_j = (\bar{\Delta}_x, \bar{\Delta}_y, \bar{\Delta}_z)$. $x_j = (x, y, z)$ are axes of Cartesian coordinate system. The other physical fields are filtered similarly.

Let us present all the variables of the problem as the sum of a filtered (large scale) and unfiltered (small scale) component: $u = \bar{u} + u'$, $B = \bar{B} + B'$, $p = \bar{p} + p'$ etc., with u_j , B_j the velocity and magnetic induction components, and p the pressure.

To simplify the modeled equations describing compressible MHD flows, it is convenient to use mass-weighted filtering (also known as Favre filtering) so as to avoid the appearance of additional SGS terms. It is determined as follows:

$$\tilde{f} = \frac{\overline{\rho f}}{\bar{\rho}}, \tag{3}$$

with ρ the density. The overline in Eq. (3), denotes ordinary filtering while the tilde denotes mass-weighted filtering. Mass-weighted filtering is used for all physical variables other than the pressure, density, and magnetic fields.

The Favre filtered velocity takes the following form

$$\tilde{u}_j = \frac{\overline{\rho u_j}}{\bar{\rho}} = \frac{\int_a^b \rho u_j G(x_j - x'_j, \bar{\Delta}_j) dx'_j}{\int_a^b \rho(x'_j) G(x_j - x'_j, \bar{\Delta}_j) dx'_j}. \tag{4}$$

³For an innovative filtering approach based on wavelet transforms and adaptive mesh refinement see De Stefano and Vasilyev (2013)

The Favre filtered quantities can be presented in the form of a sum, for instance for the velocity: $u = \tilde{u} + u''$, where the double prime designates the small-scale component.

The Favre-filtered MHD equations take the following form (Chernyshov et al. 2006a):

– *filtered continuity equation*

$$\frac{\partial \bar{\rho}}{\partial t} + \frac{\partial \bar{\rho} \tilde{u}_j}{\partial x_j} = 0; \tag{5}$$

– *filtered momentum conservation equation*

$$\frac{\partial \bar{\rho} \tilde{u}_i}{\partial t} + \frac{\partial}{\partial x_j} \left(\bar{\rho} \tilde{u}_i \tilde{u}_j + \bar{p} \delta_{ij} - \frac{1}{Re} \tilde{\sigma}_{ij} + \frac{\bar{B}^2}{2M_a^2} \delta_{ij} - \frac{1}{2M_a^2} \bar{B}_j \bar{B}_i \right) = - \frac{\partial \tau_{ji}''}{\partial x_j}; \tag{6}$$

– *filtered induction equation*

$$\frac{\partial \bar{B}_i}{\partial t} + \frac{\partial}{\partial x_j} (\tilde{u}_j \bar{B}_i - \tilde{u}_i \bar{B}_j) - \frac{1}{R_m} \frac{\partial^2 \bar{B}}{\partial x_j^2} = - \frac{\partial \tau_{ji}^b}{\partial x_j}, \tag{7}$$

as

$$\begin{aligned} \overline{\eta B_j} - \bar{\eta} \bar{B}_j &= 0, \\ \bar{\sigma}_{ij} - \tilde{\sigma}_{ij} &= 0, \end{aligned}$$

– where

$$\begin{aligned} \tilde{\sigma}_{ij} &= 2\tilde{\mu} \tilde{S}_{ij} - \frac{2}{3} \tilde{\mu} \tilde{S}_{kk} \delta_{ij} + \tilde{\zeta} \tilde{S}_{kk} \delta_{ij}, \\ \bar{\sigma}_{ij} &= 2\overline{\mu S_{ij}} - \frac{2}{3} \overline{\mu S_{kk} \delta_{ij}} + \overline{\zeta S_{kk} \delta_{ij}}, \end{aligned}$$

- and ρ —density; p —pressure; u_j —velocity in direction x_j ;
- $\sigma_{ij} = 2\mu S_{ij} - \frac{2}{3} \mu S_{kk} \delta_{ij} + \zeta S_{kk} \delta_{ij}$ —viscous stress tensor;
- $S_{ij} = 1/2(\partial u_i / \partial x_j + \partial u_j / \partial x_i)$ —strain rate tensor;
- μ —dynamic viscosity; ζ —bulk viscosity;
- δ_{ij} —the Kronecker delta; ε_{ijk} —the Levi-Civita symbol;
- $\eta = c^2 / 4\pi \sigma$ —magnetic diffusion; σ —specific electric conductivity;
- $F_l = \varepsilon_{ijk} j_j B_k / c$ —Lorentz force; B —magnetic field; j —current density.

$Re = \rho_0 u_0 L_0 / \mu_0$ is the Reynolds number, $R_m = u_0 L_0 / \eta_0$ —the magnetic Reynolds number. $M_s = u_0 / c_s$ the Mach number, $M_a = u_0 / u_a$ —the magnetic Mach number, and c_s is sound speed determined by the relation: $c_s = \sqrt{\gamma p_0 / \rho_0}$; u_a is the Alfvén speed, $u_a = B_0 / \sqrt{4\pi \rho_0}$. The bulk coefficient of viscosity ζ is neglected.

The terms on the right-hand-side of Eqs. (6)–(7) designate the influence of the SGS terms on the filtered component:

$$\tau_{ij}'' = \bar{\rho} (\tilde{u}_i \tilde{u}_j - \tilde{u}_i \tilde{u}_j) - \frac{1}{M_a^2} (\overline{B_i B_j} - \bar{B}_i \bar{B}_j); \tag{8}$$

$$\tau_{ij}^b = \overline{u_i B_j} - \tilde{u}_i \bar{B}_j - \overline{B_i u_j} - \bar{B}_i \tilde{u}_j. \tag{9}$$

Note that compressibility alters the form of the SGS stress tensor τ_{ij}'' but the magnetic SGS tensor τ_{ij}^b is the same as for incompressible MHD. The SGS-scale hydrodynamic pressure is typically neglected in the filtered equations for compressible, neutral flows with low Mach numbers (Piomelli 1999; Zang et al. 1992). By extension, the SGS magnetic pressure is also neglected in Eq. (8). However, attempts are being made at more general models.

For example, Grete et al. (2015) incorporate the full SGS strain rate tensors, including the symmetric components that account for SGS kinetic and magnetic pressure.

Let us consider the filtered equations (5)–(7) in more detail. As far as the small-scale velocity (and the other flow variables) $u'' = u - \tilde{u}$ is unknown; it has to be estimated with the use of the large-scale velocity obtained by means of filtration. Theoretically, there is no functional dependence between the small-scale velocity u'' and the large-scale one \tilde{u} , so any estimation of u'' will contain error. DNS can sometimes be used to estimate this error but this can only be carried out for relatively low Reynolds numbers due to limited computational resources.

Thus, the filtered system of MHD equations contains the unknown turbulent tensors τ_{ij}^u and τ_{ij}^b . The task of the SGS model is to express these unknown tensors in terms of the filtered flow components \tilde{u}_i and \bar{B}_i using some sort of turbulent closure (parameterizations). Ideally, the closure model should capture such effects as the Richardson turbulent cascade.

Let us consider closures for τ_{ij}^u and τ_{ij}^b . To guarantee the non-negativity of subgrid energy, these tensors must satisfy some conditions, called realizability conditions. A necessary and sufficient condition of non-negativity is provided by the positiveness of the semidefinite form for the turbulent tensors τ_{ij} such that:

$$\begin{aligned} \tau_{ii} &\geq 0 && \text{for } i \in \{1, 2, 3\}, \\ |\tau_{ij}| &\leq \sqrt{\tau_{ii}\tau_{jj}} && \text{for } i, j \in \{1, 2, 3\}, \\ \det(\tau_{ij}) &\geq 0. \end{aligned} \tag{10}$$

Let us assume that the form of the turbulent tensor τ_{ij}^u is analogous to the viscous stress tensor (eddy viscosity model), while τ_{ij}^b is analogous to ohmic dissipation. This yields:

$$\tau_{ij}^u - \frac{1}{3}\tau_{kk}^u\delta_{ij} = -2\nu_t \left(\tilde{S}_{ij} - \frac{1}{3}\tilde{S}_{kk}\delta_{ij} \right), \tag{11}$$

$$\tau_{ij}^b - \frac{1}{3}\tau_{kk}^b\delta_{ij} = -2\eta_t \bar{J}_{ij}, \tag{12}$$

where

$$\tilde{S}_{ij} = \frac{1}{2} \left(\frac{\partial \tilde{u}_i}{\partial x_j} + \frac{\partial \tilde{u}_j}{\partial x_i} \right)$$

is the large-scale strain rate tensor;

$$\bar{J}_{ij} = \frac{1}{2} \left(\frac{\partial \bar{B}_i}{\partial x_j} - \frac{\partial \bar{B}_j}{\partial x_i} \right)$$

is a large-scale magnetic rotation tensor. Here ν_t and η_t are scalar turbulent diffusion coefficients that may in general depend on the spatial coordinates and time.

In the right-hand side of Eqs. (11) and (12) the symmetric terms of the magnetic rate-of-strain tensor:

$$\bar{S}_{ij}^b = (\partial \bar{B}_i / \partial x_j + \partial \bar{B}_j / \partial x_i) / 2,$$

and vorticity tensor:

$$\bar{J}_{ij}^u = (\partial \tilde{u}_i / \partial x_j - \partial \tilde{u}_j / \partial x_i) / 2$$

are omitted, because their contribution is negligible in many circumstances (Müller and Carati 2002a). However, Grete et al. (2015) have incorporated these symmetric terms and find that they may be important in particular for supersonic flow regimes, as encountered, for

example, in the interstellar medium. We note again that the main purpose of SGS modeling is not to fully reconstruct the information lost due to filtration but rather to accurately capture the influence of the SGS flow on the large-scale energy distribution and transport.

Often the term $\frac{1}{3}\tau_{kk}^u\delta_{ij}$ is combined with the thermodynamic pressure, $\nabla(p + \frac{2}{3}k\delta_{ij})$, where $k = (\tau_{11} + \tau_{22} + \tau_{33})/2$ is the SGS turbulent kinetic energy (Erlebacher et al. 1992). In the present paper we consider the isotropic component explicitly, though the isotropic component of the magnetic tensor (12) vanishes because of vanishing J_{ii}). The isotropic component of τ^u can be found from the realizability conditions (10), which give

$$\tau_{12}^2 + \tau_{13}^2 + \tau_{23}^2 \leq \tau_{11}\tau_{22} + \tau_{11}\tau_{33} + \tau_{22}\tau_{33} \quad (13)$$

By using (11), we obtain the following expression for the isotropic component of τ^u

$$k \geq \frac{1}{2}\sqrt{3}(v_t|S^u|), \quad (14)$$

where $|\tilde{S}^u| = (2\tilde{S}_{ij}^u\tilde{S}_{ij}^u)^{1/2}$. The anisotropic and isotropic components of τ^u can then be obtained from Eqs. (11) and (14).

Different closures for the compressible MHD equations were developed by Chernyshov et al. (2006b) and further analyzed by Chernyshov et al. (2007). LES of MHD turbulence were compared with DNS and it was shown that the five closure models considered provide sufficient dissipation of kinetic and magnetic energy at comparatively low computational expense.

The effects of heat conduction were considered by Chernyshov et al. (2006c, 2008a) who developed models for the SGS terms in the energy equation as well as for the magnetic terms in the momentum and induction equations. LES of decaying MHD turbulence were performed and their greater efficiency compared to DNS was demonstrated. SGS models were similarly validated for studies of self-similar regimes in forced turbulence by Chernyshov et al. (2010, 2012). Further work on the LES of compressible MHD turbulence focused on the local interstellar medium (Chernyshov et al. 2008b) and the kurtosis and flatness of the turbulent flow (Chernyshov et al. 2009). For a comprehensive review of SGS modeling see Chernyshov et al. (2014).

Other models can be developed, using for example expressions deriving from the integro-differential equations for energy spectral density in the framework of two-point closures of turbulence like the Eddy Damped Quasi Normal Markovian closure (Chollet and Lesieur 1981). Newer versions have seen several developments implemented, such as (see Baerenzung et al. 2011 and references therein): (i) including both eddy diffusivities (viscosity and resistivity) as well as eddy noise; indeed, the effect of the small scales on the large scales is potentially a dissipation of energy (although eddy diffusivities can be negative) as well as a stochastic forcing; (ii) adapting to spectra that differ from the classical (Kolmogorov 1941) law, a feature that can be useful in the presence of magnetic fields, rotation or stratification, i.e. when the resulting energy spectra may be in a weak turbulence regime due to wave-eddy interactions; and (iii) including in these two types of coefficients the effect of helicity (velocity-vorticity correlations) as encountered in tropical cyclones or in the Planetary Boundary Layer. Helicity can be created by a combination of rotation and stratification and can play a role in the generation of large-scale magnetic fields.

In fact, in MHD, there are two other helical fields that can be defined, namely the cross-correlation between the velocity and the magnetic induction, and the magnetic helicity (correlation between vector potential and magnetic induction in three space dimensions); their effect on the large-scale dynamics of MHD flows has been considered in Yokoi (2013) where the role of cross-correlation on turbulent reconnection is particularly stressed (see also Yokoi and Yoshizawa 1993).

There are other types of LES that have been developed. Of particular note are implicit LES (ILES) methods that do not include any explicit SGS model but do include intrinsic dissipation and dispersion due to the nature of the numerical algorithm. These methods received much attention at the workshop and make up a growing fraction of astrophysical and geophysical turbulence simulation. Their primary attraction is maximal resolution; dissipation operates only at the grid scale, leaving larger scales essentially free of artificial diffusion. However, it can be difficult to assess the influence of the dissipation scheme on the properties of the resolved flow, particularly in the case of MHD where nonlinear spectral interactions are intrinsically nonlocal. For further details on ILES see Grinstein et al. (2011) and Schmidt (2015).

Another possibility that has been tested in two dimensions in MHD in a pseudo-spectral code is to decimate Fourier modes after a given cut-off scale (Meneguzzi et al. 1996); the rationale behind such a decimation, whereby for example half the modes are taken for Fourier shells beyond the chosen cut-off (and the method can be iterated), is that there are $4\pi k^2$ modes of characteristic wavenumber k , i.e. a large number at small scales; it is to be expected that their role is statistical (and with a stochastic component) and that therefore these modes do not have to be all treated explicitly. For example, in a computation with 3072^3 grid points and with a de-aliasing using a $2/3$ rule, the ratio of maximum to minimum wave numbers is 1024. Of the $27^+ \times 10^9$ modes in such a computation, half of them (or roughly 13 billions) are for wave numbers $k \geq 710$, with $\approx 12 \times 10^6$ in the very last Fourier shell (of unit width) alone (Marino et al. 2013).

In conclusion, it has been suggested that a possible future methodology to tackle complex turbulent flows as found in astrophysics and space physics might be to combine multiple approaches, including ILES, explicit SGS modeling, and also adaptive mesh refinement (Woodward et al. 2006a; De Stefano and Vasilyev 2013; Schmidt 2015)

5 Applications

In this section we briefly consider several applications of LES in MHD of relevance to astrophysics and space physics in order to highlight both the successes and the challenges of the field.

5.1 Realistic LES of Solar Granulation

A prime example demonstrating the success of LES is solar granulation. This includes in particular the uppermost visible surface of the solar convection zone where radiation transport and time-dependent ionization are important. Following the early work (Spiegel 1971, 1972; Gough et al. 1976; Toomre et al. 1976) on compressible stellar convection in the 1970s, Nordlund (1982, 1985) pioneered the field of realistic convection simulations of the solar surface, which has since advanced considerably (Stein and Nordlund 1989, 1998; Steffen et al. 1989; Wedemeyer et al. 2004; Vögler et al. 2005; Rempel 2014). These simulations employ a tabulated equation of state together with fully nonlocal radiation transfer and realistic opacities. They used different combinations of subgrid scale modeling including Smagorinsky viscosity, shock-capturing viscosities, hyperviscosities, Riemann solvers, monotonicity schemes, etc., which can be classified as implicit LES (ILES).

Simulations of solar surface convection reproduce solar observations remarkably well, both qualitatively and quantitatively. An example is shown in Fig. 5. The intensity contrast in the simulated granules is about 16 %, which agrees with the observed contrast of about

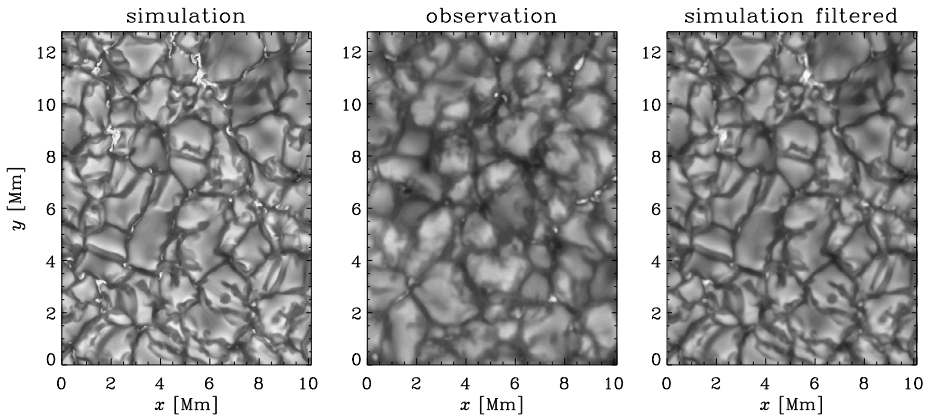


Fig. 5 Comparison between a granulation pattern from a simulation with 12 km grid size (*left*), an observed granulation pattern from the Swedish 1-meter Solar Telescope at disk center (*middle*), and the simulated one after convolving with the theoretical point spread function of a 1 meter telescope. The simulation images are for wavelength integrated light intensity while the observed image is for a wavelength band in the near UV. The image was taken on 23 May 2010 at 12:42 GMT with image restoration by use of the multi-frame blind de-convolution technique with multiple objects and phase diversity (van Noort et al. 2005). Courtesy of V.M.J. Henriques and G.B. Scharmer and adapted from Brandenburg and Nordlund (2011)

10 % after taking atmospheric seeing and the telescope point spread function into account (Stein and Nordlund 1998). Other quantitative successes include power spectra, spectral line formation, acoustic mode excitation, and local dynamo action (Nordlund et al. 2009; Rempel 2014).

An important question is to what extent the success of these simulations is due to the ILES technique employed, or to aspects of the physics that make this application particularly amenable to LES modeling. For example, the strong density stratification makes convection highly anisotropic, with a dilution of vorticity tending to “laminarize” upflows while the dynamics of the downflows are controlled mainly by buoyancy and entrainment. So, details such as the forward transfer of kinetic energy into the dissipation scale are not specifically tested. Furthermore, near the visible surface, the radiative diffusivity is large enough that no SGS model is needed for the internal energy equation. Thus, a key component of the dynamics is effectively captured through DNS. This may also account for the success of geodynamo models, which are able to run with a realistic value for the magnetic diffusivity, relegating SGS to the velocity field alone (Glatzmaier 2002; Jones 2011).

5.2 The Bottleneck Effect in HD Turbulence

Incompressible forced turbulence simulations have been carried out at resolutions up to 4096^3 meshpoints (Kaneda et al. 2003). A surprising result from this work is a strong bottleneck effect (Falkovich 1994) near the dissipative subrange, and possibly a strong inertial range correction of about $k^{-0.1}$ to the usual $k^{-5/3}$ inertial range spectrum. Interestingly, similarly strong inertial range corrections have also been seen in simulations using a Smagorinsky subgrid scale model (Haugen and Brandenburg 2006) using 512^3 meshpoints; see the dashed line in Fig. 6. Here we also show the results of simulations with hyperviscosity, i.e. the $\nu \nabla^2$ diffusion operator has been replaced by a $\nu_3 \nabla^6$ operator (Haugen and Brandenburg 2004), also with 512^3 meshpoints (dash-dotted line). Hyperviscosity greatly exaggerates the bottleneck effect, but it does not seem to affect the inertial range significantly; see Fig. 6.

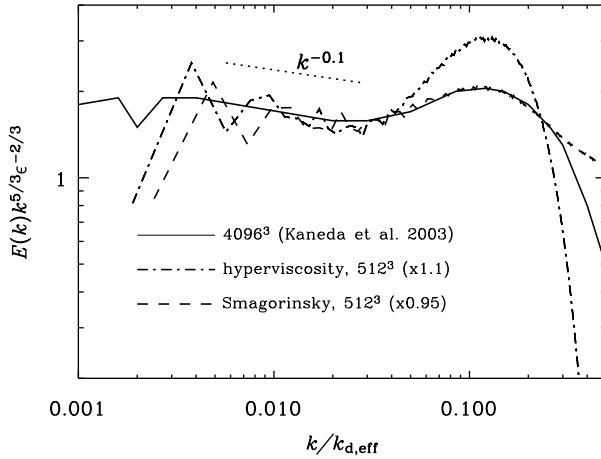


Fig. 6 Comparison of energy spectra of the 4096^3 meshpoints run (Kaneda et al. 2003), solid line, and 512^3 meshpoints runs with hyperviscosity (dash-dotted line) and Smagorinsky viscosity (dashed line). (In the hyperviscous simulation we use $\nu_3 = 5 \times 10^{-13}$.) The Taylor microscale Reynolds number of the Kaneda simulation is 1201, while the hyperviscous simulation of Haugen and Brandenburg (2004) has an approximate Taylor microscale Reynolds number of $340 < Re_\lambda < 730$. For the Smagorinsky simulation the value of Re_λ is slightly smaller. Courtesy of Nils E. Haugen (Haugen and Brandenburg 2006)

Woodward et al. (2006a,b) found a similar bottleneck effect in ILES of homogeneous, decaying, sonic turbulence (Mach number 1). Furthermore, they implemented a nonlinear SGS model (mentioned previously in Sect. 4) designed to supplement the numerical dissipation and they found that the combined ILES+SGS model could both alleviate the bottleneck effect and reproduce the spectrum of higher-resolution ILES across much of the resolved dynamical range.

If the details of the inertial range spectrum are sensitive to the dissipation even in this most fundamental of applications then what should we expect for more complex flows? Does this call into question the *central premise* discussed in Sect. 1, that the dynamics of the large scales can be reliably captured despite the challenges of modeling the SGS physics?

5.3 Problems in Dynamo Theory

5.3.1 Small-Scale Dynamoes

Unlike many industrial applications where LES have been tested against experiments, this is currently impossible for hydromagnetic flows exhibiting dynamo action. Except for astrophysical dynamoes, there are not even a hand-full of laboratory experiments to date that produce self-excited hydromagnetic dynamo action. Therefore, an important benchmark is provided by DNS.

Dynamoes come in two flavors: small-scale and large-scale dynamoes (see Brandenburg and Subramanian 2005; Brandenburg et al. 2012, for recent reviews). In the kinematic phase, during which the magnetic field grows exponentially from a weak seed magnetic field, the magnetic field exhibits a $k^{3/2}$ (Kazantsev 1968) spectrum. Evidently, this spectrum diverges toward small length scales, so one cannot expect to obtain the correct growth rate with LES. This has consequences for understanding the excitation conditions of small-scale dynamoes. DNS have demonstrated that the onset of small-scale dynamo action depends on the value

of the magnetic Prandtl number (see Isakov et al. 2007 and Brandenburg 2011 for the classical incompressible case and Federrath et al. 2014 for the case of supersonic turbulence). Meanwhile, the magnetic Prandtl number does not enter into traditional LES, so this question cannot be addressed. This is also the case for the magneto-rotational instability (MRI), which has been shown to be sensitive to the value of the magnetic Prandtl number.

As the small-scale dynamo saturates, the peak of magnetic energy moves gradually toward larger scales, so there is a chance that this can be modeled with LES. However, simulations using a Smagorinsky-like magnetic diffusivity prescription have yielded saturation field strengths that are significantly below those obtained with DNS (Haugen and Brandenburg 2006). This shortcoming might be related to not yet being in the asymptotic regime in which *both* magnetic and kinetic Reynolds numbers are large enough. A similar situation might apply to the ratio of kinetic to magnetic energy dissipation, which is known to scale with magnetic Prandtl number to a power that is around 0.6. Again, LES are not currently able to shed any light on this, because the magnetic Prandtl number does not enter in standard subgrid scale models. Addressing this deficiency is a difficult but perhaps auspicious challenge in need of further research.

5.3.2 Large-Scale Dynamos

Large-scale dynamos produce magnetic fields whose scale exceed that of the turbulent eddies. They are believed to be relevant for understanding the global 22-year cycle of the Sun's magnetic field, and similar large-scale magnetic fields in other astrophysical bodies. A leading theory for understanding large-scale dynamos is mean-field theory which explains the occurrence of correlation in the mean electromotive force that has a component parallel to the mean magnetic field. This is generally referred to as the α effect, is typically related to the presence of helicity in the system. However, DNS have shown that its magnitude is reduced with increasing values of the microphysical magnetic Reynolds number (Cattaneo and Hughes 1996). This is now generally referred to as catastrophic quenching and has to do with a magnetic contribution to the α effect, which is proportional to the current helicity of the fluctuating field, $\overline{\mathbf{j} \cdot \mathbf{b}}$. Here, $\mathbf{j} = \nabla \times \mathbf{b} / \mu_0$ is the current density of the fluctuating magnetic field, \mathbf{b} . It is in turn related to the magnetic helicity of the small-scale field, $\overline{\mathbf{a} \cdot \mathbf{b}}$, where \mathbf{a} is the magnetic vector potential of $\mathbf{b} = \nabla \times \mathbf{a}$. It obeys the evolution equation

$$\frac{\partial}{\partial t} \overline{\mathbf{a} \cdot \mathbf{b}} = -\overline{\mathbf{u} \times \mathbf{b} \cdot \mathbf{B}} - 2\eta\mu_0 \overline{\mathbf{j} \cdot \mathbf{b}} - \nabla \cdot (\overline{\mathbf{e} \times \mathbf{a}}), \quad (15)$$

Here, $\overline{\mathbf{u} \times \mathbf{b}}$ is the mean electromotive force, η is the microphysical magnetic diffusivity, and $\overline{\mathbf{e} \times \mathbf{a}}$ is the magnetic helicity flux, where \mathbf{e} is the fluctuating electric field. We shall now discuss two aspects of this equation that are relevant to LES.

First, if the system is homogeneous, i.e., there are no boundaries and no large-scale variations of turbulent intensity and helicity across the system, the divergence of the magnetic helicity flux vanishes. In that case, there must be a balance between the first two terms on the right-hand side of Eq. (15). Although the assumption of homogeneity is only of academic interest, it does provide a test case that must be obeyed equally by DNS and LES. In particular, replacing the microphysical diffusion by hyperdiffusion changes the scale dependence of the $\overline{\mathbf{j} \cdot \mathbf{b}}$ term and has been shown to exaggerate the amplitude of the large-scale field relative to that of the small-scale field (Brandenburg and Sarson 2002). This phenomenon is well understood, but it would still be of interest to experiment with other representations of small-scale magnetic dissipation to see how the large-scale magnetic field is being artificially modified by the numerical representation of the small-scale physics.

Secondly, in the inhomogeneous case, magnetic helicity fluxes are possible. In principle, these fluxes are gauge-dependent, and would thus be unphysical. If, in the statistically steady state, the time derivative of $\overline{\mathbf{a} \cdot \mathbf{b}}$ on the left-hand side of Eq. (15) vanishes, we have

$$0 = -2\overline{\mathbf{u} \times \mathbf{b} \cdot \mathbf{B}} - 2\eta\mu_0\overline{\mathbf{j} \cdot \mathbf{b}} - \nabla \cdot (\overline{\mathbf{e} \times \mathbf{a}}), \quad (16)$$

which implies that $\nabla \cdot (\overline{\mathbf{e} \times \mathbf{a}})$ is now balanced by terms that are manifestly gauge-independent. This is a remarkable property that allows us to measure the magnetic helicity flux divergence. This has been done in several recent papers (Mitra et al. 2010; Hubbard and Brandenburg 2010; Del Sordo et al. 2013). Interestingly, it turns out that the $\nabla \cdot (\overline{\mathbf{e} \times \mathbf{a}})$ remains subdominant for all simulations performed so far, and that only at the largest resolution available so far, it becomes approximately equal to the $2\eta\mu_0\overline{\mathbf{j} \cdot \mathbf{b}}$ term. Here, the magnetic Reynolds number based on the wavenumber of the energy-carrying eddies is about 1000, which is still barely achievable in DNS.

It is at present unclear whether LES are able to lead to meaningful insight into the regime of larger magnetic Reynolds numbers. One practical difficulty in determining $\overline{\mathbf{e} \times \mathbf{a}}$ is the computation of the magnetic vector potential, which is not always readily available.

5.4 Astrophysical Turbulence and MRI

Most astrophysical plasmas are highly compressible. Thus, capturing the influence of shocks is essential. Since the viscous scale in shocks is far too small to be resolved, DNS is not possible so modelers must turn to LES. All shock-capturing astrophysical codes include some sort of subgrid-scale model, whether it be an explicit artificial viscosity (e.g. Stone and Norman 1992) or an implicit numerical dissipation that arises through a Riemann solver as in Godunov-type methods (e.g. Roe 1986; LeVeque 2002). These methods have been used for over 50 years, and there is no question this approach works extremely well.

Developing more sophisticated SGS models for turbulence in highly compressible astrophysical plasmas will be a formidable challenge. A complete understanding of how shocks and contact discontinuities interact with the turbulent cascade and affect small scales is still lacking and is a major research problem in its own right.

One very important example of astrophysical turbulence in which compressibility does not play an essential role is the magnetorotational instability, or MRI (Balbus and Hawley 1991). MRI-induced turbulence is thought to dominate the energy and angular momentum transport in magnetized accretion disks (Balbus and Hawley 1998).

The MRI is a particularly important case study for LES of MHD turbulence because the role of artificial dissipation has been closely scrutinized in recent years. This scrutiny began with an influential paper by Fromang and Papaloizou (2007) that demonstrated a decrease in the amplitude of the MRI-induced turbulent stresses with increasing spatial resolution for the specific case of a local shearing box with no net flux through the layer. The potential implications were profound; If this trend were to continue to the dynamic ranges active in actual accretion disks, then the turbulent transport would be drastically less efficient than previously thought and insufficient to account for the outward angular momentum transport necessary to sustain the accretion process (Balbus and Hawley 1998). They attributed this behavior to the form of the numerical diffusion and its interaction with the source terms that sustain the instability. Other LES simulations soon confirmed this result for similar model configurations and demonstrated that the decrease in turbulent stresses with increasing resolution does not occur when explicit diffusion is included (see Bodo et al. 2011, and references therein).

However, after nearly eight years of active research, it appears that this “convergence problem” is not as serious as initially thought; the problem appears to be a symptom of this particular model setup and goes away when other model configurations are considered. For example, if the vertical extent of the computational domain is increased so that it is twice as large as the horizontal extent, the convergence problem goes away, the turbulent stresses increase by an order of magnitude, and the Fourier power spectrum is altered substantially. Furthermore, the convergence problem does not arise for shearing boxes with a background density stratification and/or a net magnetic flux through the layer (e.g. Fromang 2013; Turner et al. 2014).

In the no-net-flux case, the MRI must sustain a shear dynamo and it may be that the properties of this dynamo (which is a macroscopic flow related to the outer scale of the turbulence) is not properly captured in small boxes and this introduces an artificial dependence on SGS diffusion. Further insight into why the MRI behaves so differently in small, non-stratified, shearing boxes with no net flux requires a deeper understanding of the MRI-driven dynamo, possibly based on reduced models. This deeper understanding is also needed to account for the magnetic cycles found in the larger boxes (see Fromang 2013; Turner et al. 2014).

Furthermore, direct measurement of turbulent resistivity in the MRI by three different groups all find the same result, using very different codes and Reynolds numbers (Guan and Gammie 2009; Lesur and Longaretti 2009; Fromang and Stone 2009). The turbulent magnetic Prandtl number is close to one, which implies the resistivity is very large (of order $u\ell$, where u and ℓ are characteristic turbulent velocity and length scales; this implies that the turbulent magnetic Reynolds number is much smaller than that given by the Ohmic resistivity). This argues that macroscopic (turbulent) effects are more important than microscopic diffusivities, which in turn argues that the MRI is not sensitive to SGS physics.

Further confidence in the ILES approach to modeling MRI turbulence comes from the recent study by Meheut et al. (2015). They compared lower-resolution ILES to high-resolution DNS and found good agreement, at least for the special case of a non-zero mean field and a low magnetic Prandtl number, meaning that the magnetic diffusion was captured explicitly while the kinetic energy dissipation was relegated to the numerical diffusion. In particular, the kinetic and magnetic power spectra at low to intermediate wavenumbers in a DNS with resolution (800, 1600, 832) were well reproduced by ILES runs with resolutions of order 128^3 and 256^3 at a fraction of the computational expense.

If, on the other hand, one wishes to construct explicit SGS models for LES of MRI, it may prove beneficial to exploit the potential magnetic induction introduced by Salhi et al. (2012), $\mathbf{B} \cdot \nabla \Theta$, where Θ is the potential temperature. This is an analogue of the potential vorticity which, unlike the potential vorticity, is a Lagrangian invariant for a magnetized, Boussinesq fluid.

5.5 Hybrid Kinetic-MHD Models

In Sect. 3.4 we emphasized that the small-scale dynamics of a plasma flow are often not well represented by MHD. This is particularly the case for low-density plasmas such as the solar wind or Earth’s magnetosphere. Departures from MHD must be treated by solving the kinetic equations in some form, often with simplifying assumptions designed to mitigate the computational requirements. See Sect. 3.4 for further details and for a survey of some applications from solar and space physics.

Many other astrophysical flows require a kinetic-MHD description to capture the essential physics. Here there is no question that SGS physics is important. For example,

anisotropic conduction and viscosity on small scales can influence the large-scale dynamics through the magneto-thermal and magneto-viscous instabilities (Balbus 2000, 2001; Quataert et al. 2002). There is some hope that hybrid PIC simulations of small scales will be able to provide a reasonable SGS model (including coefficients of conduction and viscosity) that can be used in kinetic MHD models of various astrophysical problems including the MRI (see Sect. 5.4), hot gas in galaxy clusters, and turbulence in the interstellar medium.

During the GTP workshop, W. Schmidt described a promising hierarchical approach for including small-scale kinetic reconnection effects as an SGS model in MHD simulations. The approach is similar to self-consistent mean-field dynamo theory but encompasses three stages:

1. kinetic simulations of reconnection and dissipation providing effective transport coefficients (e.g., the turbulent EMF α and β coefficients) to account for kinetic plasma processes;
2. In turn, these coefficients are to be used in non-ideal MHD simulations of turbulent dynamos and reconnection, providing a sub-grid model for stage 3;
3. quasi-ideal simulations of MHD turbulence.

6 Summary and Outlook

The diverse applications surveyed in Sect. 5 all have at least two things in common. First, these systems are well described on large scales by the equations of MHD and second, they are characterized by turbulent parameter regimes that are inaccessible to DNS. Computers simply are not capable of modeling all relevant scales from the macroscopic scales to the Larmor radius. Thus, in order to model such systems it is absolutely essential that we adopt an LES approach.

For many systems it may be sufficient to simply minimize the artificial dissipation through the use of numerical methods that include their own intrinsic dissipation. Such methods, often referred to generally as implicit LES (though see Grinstein et al. 2011, for a more precise definition of ILES), maximize a simulation's dynamic range for a given spatial resolution by confining the artificial dissipation to scales comparable to the grid spacing.

Other applications may be more subtle. For these, it may be necessary to model the subgrid-scale physics more reliably in order to accurately capture the dynamics of the larger scales. This can be achieved by applying a formal filtering procedure to the governing equations (Sect. 4) and then introducing parameterized or tabulated SGS models based on theoretical and phenomenological arguments or on local simulations that capture the small-scale plasma physics.

When devising SGS models for MHD, some guidance can be provided by the much more mature field of LES/SGS modeling in turbulent HD (non-magnetic) flows, which has received much attention particularly in the context of atmospheric and engineering applications (Sagaut 2006), with a growing body of literature also on highly compressible astrophysical flows (Schmidt 2015). Still, as discussed in Sects. 2–3, MHD possesses its own unique challenges.

Some of the challenges in representing SGS physics arise from the nature of the MHD equations themselves. The presence of magnetism in a turbulent, electrically conducting fluid introduces an intrinsic anisotropy to the flow that becomes more pronounced with decreasing scale (Sect. 3). The small-scale flow is also intrinsically inhomogeneous, marked by intermittent patches of enhanced dissipation and magnetic reconnection in current sheets.

This small-scale dissipation and reconnection can heat the plasma and reshape the large-scale magnetic topology. Other factors that can influence the coupling between large and small scales include magnetic helicity, cross helicity, dynamic alignment, and the suppression of small-scale turbulence by large-scale magnetic flux (Sect. 2.2). Most of these effects are neglected by current SGS models, which often assume some degree of isotropy and homogeneity to make paramphenomenaeterizations more tractable. Further investigation of these issues and associated SGS model development is sorely needed. Help in dealing with inhomogeneity and intermittency may also come from adaptive mesh refinement (AMR), which was auspiciously addressed at the GTP Workshop by O. Vasilyev (De Stefano and Vasilyev 2013).

Yet, the challenges in modeling SGS physics do not stop there. In most plasma flows (particularly those with low density), the MHD equations cease to be valid on the smallest scales, giving rise to kinetic effects that lie outside the scope of ideal or even resistive MHD. Such effects may regulate the dissipation of energy and magnetic helicity, the associated plasma heating, and the restructuring of the magnetic topology through magnetic reconnection. Kinetic effects also introduce new phenomena that may influence large-scale dynamics, including non-thermal particle acceleration and anisotropic heat conduction and viscosity. A promising path forward is to couple MHD models to kinetic or hybrid codes that capture some of the relevant kinetic effects (Sect. 3.4, 5.5). But this will not be easy; it is a formidable theoretical and computational challenge.

As mentioned several times in this review, a promising way to validate LES models in MHD and to guide their development is to compare them with higher-resolution DNS or ILES. Preliminary results from astrophysical application have generally been promising (Grete et al. 2015; Meheut et al. 2015) but more work is needed. Kinetic and hybrid simulations can also be used to motivate and assess SGS models, particularly for models that are not purely dissipative. We expect to see much progress on these fronts in the next 5–10 years.

There is no oracle or omen to tell you whether your application requires sophisticated SGS modeling or if ILES is sufficient. This judgment must be made on a case-by-case basis grounded on a thorough understanding of the underlying physics and indeed, it is still being assessed even for the relatively well-established problems surveyed in Sect. 5. Though there are robust features of MHD turbulence that can be exploited in SGS models, many aspects of the SGS physics are likely not universal. Yet, if prudence is followed when designing numerical models and interpreting the results, current applications do give us confidence in the central premise of LES (Sect. 1), namely that real heliophysical and astrophysical systems can be meaningfully modeled when only a fraction of the dynamically active scales are explicitly resolved. LES of MHD turbulence is a still a nascent field, brimming with challenges...and opportunities.

Acknowledgements We thank the reviewer Wolfram Schmidt and also Hideyuki Hotta for constructive comments that have improved the content and presentation of the paper. The work of A. Petrosyan was supported by the Russian Foundation for Basic Research (14-29-06065) and Program #9 of the Russian Academy of Science Presidium “Experimental and Theoretical Studies of Solar System objects and stellar planetary systems”. A. Brandenburg gratefully acknowledges support from the Swedish Research Council grants No. 621-2011-5076 and 2012-5797 and the Research Council of Norway under the FRINATEK grant No. 231444. NCAR is sponsored by the National Science Foundation.

References

- O. Agullo, W.-C. Müller, B. Knaepen, D. Carati, *Phys. Plasmas* **8**(7), 3502 (2001)
A. Alexakis, P.D. Mininni, A. Pouquet, *Phys. Rev. E* **72**, 046301 (2005)

- O. Alexandrova, J. Saur, C. Lacombe et al., *Phys. Rev. Lett.* **103**, 165003 (2009)
- J. Ambrosiano, W.H. Matthaeus, M.L. Goldstein, D. Plante, J. Geophys. Res. **93**, 14383 (1988)
- J. Baerenzung, H. Politano, Y. Ponty, A. Pouquet, *Phys. Rev. E* **77**, 046303 (2008a)
- J. Baerenzung, H. Politano, Y. Ponty, A. Pouquet, *Phys. Rev. E* **78**, 026310 (2008b)
- J. Baerenzung, P. Mininni, A. Pouquet, D. Rosenberg, *J. Atmos. Sci.* **68**, 2757 (2011)
- S.A. Balbus, *Astrophys. J.* **534**, 420 (2000)
- S.A. Balbus, *Astrophys. J.* **562**, 909 (2001)
- S.A. Balbus, J.F. Hawley, *Astrophys. J.* **376**, 214 (1991)
- S.A. Balbus, J.F. Hawley, *Rev. Mod. Phys.* **70**, 1 (1998)
- S.D. Bale, P.J. Kellogg, F.S. Mozer, T.S. Horbury, H. Reme, *Phys. Rev. Lett.* **94**, 215002 (2005)
- G.K. Batchelor, *The Theory of Homogeneous Turbulence* (Cambridge University Press, Cambridge, 1982), 197 pp.
- J.W. Belcher, L. Davis Jr., *J. Geophys. Res.* **76**, 3534 (1971)
- A.R. Bell, *Mon. Not. R. Astron. Soc.* **182**, 147 (1978)
- F. Bellet, F.S. Godeferd, J.F. Scott, C. Cambon, *J. Fluid Mech.* **562**, 83 (2006)
- A. Bhattacharjee, Y.-M. Huang, H. Yang, B. Rogers, *Phys. Plasmas* **16**, 112102 (2009)
- J. Birn, E. Priest, *Reconnection of Magnetic Fields* (Cambridge University Press, New York, 2007)
- D. Biskamp, *Phys. Fluids* **29**, 1520 (1986)
- D. Biskamp, *Magnetic Reconnection in Plasmas* (Cambridge University Press, Cambridge, 2000)
- D. Biskamp, *Magnetohydrodynamic Turbulence* (Cambridge University Press, Cambridge, 2003), 310 pp.
- G. Bodo, F. Cattaneo, A. Ferrari, A. Mignone, P. Rossi, *Astrophys. J.* **739**, 82 (2011)
- S. Boldyrev, *Phys. Rev. Lett.* **96**, 115002 (2006)
- A. Brandenburg, *Astrophys. J.* **550**, 824 (2001)
- A. Brandenburg, *Astrophys. J.* **697**, 1206 (2009)
- A. Brandenburg, *Astrophys. J.* **741**, 92 (2011)
- A. Brandenburg, *Astrophys. J.* **791**, 12 (2014)
- A. Brandenburg, O. Gressel, S. Jabbari, N. Kleeorin, I. Rogachevskii, *Astron. Astrophys.* **562**, A53 (2014), 15 pp.
- A. Brandenburg, K. Kemel, N. Kleeorin, I. Rogachevskii, *Astrophys. J.* **749**, 179 (2012)
- A. Brandenburg, A. Nordlund, *Rep. Prog. Phys.* **74**, 046901 (2011)
- A. Brandenburg, G.R. Sarson, *Phys. Rev.* **88**, 055003 (2002)
- A. Brandenburg, K. Subramanian, *Phys. Rep.* **417**, 1 (2005)
- A. Brandenburg, D. Sokoloff, K. Subramanian, *Space Sci. Rev.* **169**, 123 (2012)
- B.P. Brown, M.S. Miesch, M.K. Browning, A.S. Brun, J. Toomre, *Astrophys. J.* **732**, 69 (2011)
- C. Cambon, L. Jacquin, *J. Fluid Mech.* **202**, 295 (1989)
- C. Cambon, F.S. Godeferd, B. Favier, Incorporating linear dynamics and strong anisotropy in KS. application to diffusion in rotating, stratified, MHD turbulence and to aeroacoustics, in *New Approaches in Modeling Multiphase Flows and Dispersion in Turbulence, Fractal Methods and Synthetic Turbulence*. ERCOFTAC Series, vol. 18 (Springer, New York, 2012)
- P. Cassak, M. Shay, *Phys. Plasmas* **14**, 102114 (2007)
- F. Cattaneo, D.W. Hughes, *Phys. Rev. E* **54**, R4532 (1996)
- B.D.G. Chandran, *Astrophys. J.* **720**, 548 (2010)
- S. Chandrasekhar, *Philos. Trans. R. Soc. Lond. Ser. A* **242**, 557 (1950)
- S. Chandrasekhar, *Proc. R. Soc. Lond. Ser. A* **207**, 301 (1951)
- P. Charbonneau, *Annu. Rev. Astron. Astrophys.* **52**, 251–290 (2015)
- A.A. Chernyshov, K.V. Karelsky, A.S. Petrosyan, *Russ. J. Numer. Anal. Math. Model.* **21**(1), 1 (2006a)
- A.A. Chernyshov, K.V. Karelsky, A.S. Petrosyan, *Phys. Plasmas* **13**(3), 032304 (2006b)
- A.A. Chernyshov, K.V. Karelsky, A.S. Petrosyan, *Phys. Plasmas* **13**(10), 104501 (2006c)
- A.A. Chernyshov, K.V. Karelsky, A.S. Petrosyan, *Phys. Fluids* **19**(4) (2007)
- A.A. Chernyshov, K.V. Karelsky, A.S. Petrosyan, *Phys. Fluids* **20**(8), 085106 (2008a)
- A.A. Chernyshov, K.V. Karelsky, A.S. Petrosyan, *Astrophys. J.* **686**, 1137 (2008b)
- A.A. Chernyshov, K.V. Karelsky, A.S. Petrosyan, *Theor. Comput. Fluid Dyn.* **29**, 451 (2009)
- A.A. Chernyshov, K.V. Karelsky, A.S. Petrosyan, *Phys. Plasmas* **17**, 102307 (2010)
- A.A. Chernyshov, K.V. Karelsky, A.S. Petrosyan, *Flow Turbul. Combust.* **89**, 563 (2012)
- A.A. Chernyshov, K.V. Karelsky, A.S. Petrosyan, *Phys. Usp.* **57**, 133 (2014)
- J. Cho, E.T. Vishniac, *Astrophys. J.* **539**, 273 (2000)
- J.-P. Chollet, M. Lesieur, *J. Atmos. Sci.* **38**, 2747 (1981)
- S. Corrsin, *NACA Res. memo* 58B11 (1958)
- A. Craya, Contribution à l'analyse de la turbulence associée à des vitesses moyennes. *Pub. Sci. et Téch. du Ministère de l'Air (France)*, No. 345 (1958)
- S. Dalena, A.F. Rappazzo, P. Dmitruk, A. Greco, W.H. Matthaeus, *Astrophys. J.* **783**, 143 (2014)

- W. Daughton, V. Roytershteyn, H. Karimabadi et al., *Nat. Phys.* **7**, 539 (2011a)
- W. Daughton, V. Roytershteyn, H. Karimabadi, L. Yin, B.J. Albright, S.P. Gary, K.J. Bowers, *Modern Challenges in Nonlinear Plasma Physics*. American Institute of Physics Conference Series, vol. 1320 (2011b), p. 144
- A. Delache, C. Cambon, F.S. Godeferd, *Phys. Fluids* **26**, 025104 (2014)
- F. Del Sordo, G. Guerrero, A. Brandenburg, *Mon. Not. R. Astron. Soc.* **429**, 1686 (2013)
- G. De Stefano, O.V. Vasilyev, *J. Comp. Physiol.* **238**, 240 (2013)
- P. Dmitruk, D.O. Gomez, E.E. DeLuca, *Astrophys. J.* **505**, 974 (1998)
- P. Dmitruk, W.H. Matthaeus, N. Seenu, *Astrophys. J.* **617**, 667 (2004)
- P. Dmitruk, W.H. Matthaeus, *Phys. Rev. E* **76**, 036305 (2007)
- P. Dmitruk, W.H. Matthaeus, *Phys. Plasmas* **16**, 062304 (2009)
- M. Dobrowolny, A. Mangeney, P. Veltri, *Phys. Rev. Lett.* **45**, 144 (1980)
- J.F. Drake, M. Swisdak, H. Che, M.A. Shay, *Nature* **443**, 553 (2006)
- G. Einaudi, M. Velli, *Phys. Plasmas* **6**, 4146 (1999)
- G. Erlebacher, M. Hussaini, C. Speziale, T. Zang, *J. Fluid Mech.* **238**, 155 (1992)
- G. Falkovich, *Phys. Fluids* **6**, 1411 (1994)
- B.F.N. Favier, F.S. Godeferd, C. Cambon, A. Delache, W.J.T. Bos, *J. Fluid Mech.* **681**, 434 (2011)
- B.F.N. Favier, F.S. Godeferd, C. Cambon, *Geophys. Astrophys. Fluid Dyn.* **106**, 89 (2012)
- C. Federrath, J. Schober, S. Bovino, D.R.G. Schleicher, *Astrophys. J. Lett.* **797**, L19 (2014)
- T. Forbes, E.R. Priest, *Magnetic Reconnection: MHD Theory and Applications* (Cambridge University Press, New York, 2000). ISBN 978-0521033947
- U. Frisch, A. Pouquet, P.-L. Sulem, M. Meneguzzi, *J. Mec. Theor. Appl. Suppl.* 191–216 (1983)
- S. Fromang, J. Papaloizou, *Astron. Astrophys.* **476**, 1113 (2007)
- S. Fromang, J. Stone, *Astron. Astrophys.* **507**, 19 (2009)
- S. Fromang, in *Role and Mechanisms of Angular Momentum Transport During the Formation and Early Evolution of Stars*, ed. by P. Hennebelle, C. Charbonnel. Series EAS Publ. Ser., vol. 62 (EDP Sciences, Les Ulis, 2013), p. 95
- S. Galtier, S.V. Nazarenko, A.C. Newell, A. Pouquet, *J. Plasma Phys.* **63**, 447 (2000)
- A.V. Glazunov, V.N. Lykossov, *Russ. J. Numer. Anal. Math. Model.* **18**, 279 (2003)
- G.A. Glatzmaier, *Annu. Rev. Earth Planet. Sci.* **30**, 237–257 (2002)
- P. Goldreich, S. Sridhar, *Astrophys. J.* **438**, 763 (1995)
- P. Goldreich, S. Sridhar, *Astrophys. J.* **485**, 680 (1997)
- D.O. Gough, D.R. Moore, E.A. Spiegel, N.O. Weiss, *Astrophys. J.* **206**, 536 (1976)
- R. Grauer, J. Krug, C. Mariani, *Phys. Lett. A* **195**, 335 (1994)
- P. Grete, D.G. Vlaykov, W. Schmidt, D.R.G. Schleicher, C. Federrath, *New J. Phys.* **17**, 023070 (2015)
- F.F. Grinstein, L.G. Margolin, W.J. Rider, *Implicit Large Eddy Simulation: Computing Turbulent Fluid Dynamics* (Cambridge University Press, Cambridge, 2011), 578 pp.
- X. Guan, C.F. Gammie, *Astrophys. J.* **697**, 1901 (2009)
- G.W. Hammett, F.W. Perkins, *Phys. Rev. Lett.* **64**, 3019 (1990)
- N.E.L. Haugen, A. Brandenburg, *Phys. Rev. E* **70**, 026405 (2004)
- N.E.L. Haugen, A. Brandenburg, *Phys. Fluids* **18**, 075106 (2006)
- C.T. Haynes, D. Burgess, E. Camporeale, *Astrophys. J.* **783**, 38 (2014)
- P. Hellinger, P.M. Trávníček, *J. Geophys. Res. Space Phys.* **118**, 5421 (2013)
- J.R. Herring, *Phys. Fluids* **17**, 859 (1974)
- J.C. Higdon, *Astrophys. J.* **285**, 109 (1984)
- J.V. Hollweg, *J. Geophys. Res.* **104**, 14811 (1999)
- G.G. Howes, W. Dorland, S.C. Cowley et al., *Phys. Rev. Lett.* **100**, 065004 (2008)
- A. Hubbard, A. Brandenburg, *Geophys. Astrophys. Fluid Dyn.* **104**, 577 (2010)
- R.S. Hughes, S.P. Gary, J. Wang, *Geophys. Res. Lett.* **41**, 8681 (2014)
- P.S. Iroshnikov, *Sov. Astron.* **7**, 566 (1963)
- A.B. Isakov, A.A. Schekochihin, S.C. Cowley, J.C. McWilliams, M.R.E. Proctor, *Phys. Rev. Lett.* **98**, 208501 (2007)
- F. Jenko, W. Dorland, M. Kotschenreuther, B.N. Rogers, *Phys. Plasmas* **7**, 1904 (2000)
- J.R. Jokipii, *Astrophys. J.* **146**, 480 (1966)
- C.A. Jones, *Annu. Rev. Fluid Mech.* **43**, 583–614 (2011)
- B.B. Kadomtsev, O.P. Pogutse, *Sov. Phys. JETP* **38**, 283 (1974). See also *Zh. Eksp. Teor. Fiz.* **65**, 575 (1973)
- Y. Kaneda, T. Ishihara, M. Yokokawa, K. Itakura, A. Uno, *Phys. Fluids* **15**, L2 (2003)
- H. Karimabadi, V. Roytershteyn, M. Wan et al., *Phys. Plasmas* **20**, 012303 (2013)
- T. de Karman, L. Howarth, *Proc. R. Soc. Lond. Ser. A* **164**, 192 (1938)
- A.P. Kazantsev, *J. Exp. Theor. Phys.* **26**, 1031 (1968)

- P.J. Käpylä, A. Brandenburg, N. Kleeorin, M.J. Mantere, I. Rogachevskii, *Mon. Not. R. Astron. Soc.* **422**, 2465 (2012)
- K. Kemel, A. Brandenburg, N. Kleeorin, D. Mitra, I. Rogachevskii, *Sol. Phys.* **287**, 293 (2013)
- N.I. Kleeorin, I.V. Rogachevskii, A.A. Ruzmaikin, *Sov. Astron. Lett.* **15**(4), 274 (1989)
- Y. Klimontovich, *Phys. Usp.* **40**, 21 (1997)
- B. Knaepen, P. Moin, Center for Turbulence Research Annual Research Briefs **297** (2003)
- A.N. Kolmogorov, *Dokl. Akad. Nauk SSSR* **30**(4), 299 (1941)
- G. Kowal, A. Lazarian, E. Vishniac, K. Otmianowska-Mazur, *Astrophys. J.* **700**63 (2009)
- R.H. Kraichnan, *Phys. Fluids* **8**, 1385 (1965)
- R.H. Kraichnan, *Phys. Fluids* **10**, 1417 (1967)
- R.H. Kraichnan, *Phys. Rev.* **107**, 1485 (1958)
- R.H. Kraichnan, *J. Fluid Mech.* **59**, 745 (1973)
- F. Krause, K.H. Rädler, *Mean-Field Magnetohydrodynamics and Dynamo Theory* (Pergamon Press, Oxford, 1980)
- R.H. Kraichnan, D.C. Montgomery, *Phys. Rep.* **43**, 547 (1980)
- C. Lamribe, P.P. Cortet, F. Moisy, *Phys. Rev. Lett.* **107**, 024503 (2011)
- G. Lapenta, *Phys. Rev. Lett.* **100**, 235001 (2008)
- A. Lazarian, E. Vishniac, *Astrophys. J.* **517**, 700 (1999)
- A. Lazarian, L. Vlahos, G. Kowal, H. Yan, A. Beresnyak, E.M. de Gouveia Dal Pino, *Space Sci. Rev.* **173**, 557 (2012a)
- A. Lazarian, G.L. Eyink, E.T. Vishniac, *Phys. Plasmas* **19**, 012105 (2012b)
- E. Lee, M.E. Brachet, A. Pouquet, P.D. Mininni, D. Rosenberg, *Phys. Rev. E* **81**, 016318 (2010)
- A. Leonard, *Adv. Geophys.* **18**, 237 (1974)
- G. Lesur, P.-Y. Longaretti, *Astron. Astrophys.* **504**, 309 (2009)
- R.J. LeVeque, *Finite Volume Methods for Hyperbolic Problems* (Cambridge University Press, Cambridge, 2002), 580 pp.
- N.F. Loureiro, A.A. Schekochihin, S.C. Cowley, *Phys. Plasmas* **14**, 100703 (2007)
- N.F. Loureiro, D.A. Uzdensky, A.A. Schekochihin, S.C. Cowley, T.A. Yousef, *Mon. Not. R. Astron. Soc.* **399**, L146 (2009)
- N.F. Loureiro, R. Samtaney, A.A. Schekochihin, D.A. Uzdensky, *Phys. Plasmas* **19**, 042303 (2012)
- N.F. Loureiro, A.A. Schekochihin, D.A. Uzdensky, *Phys. Rev. E* **87**, 013102 (2013)
- S.A. Markovskii, B.J. Vasquez, C.W. Smith, J.V. Hollweg, *Astrophys. J.* **639**, 1177 (2006)
- R. Marino, P.D. Mininni, D. Rosenberg, A. Pouquet, *Phys. Rev. E* **87**, 033016 (2013)
- J. Mason, F. Cattaneo, S. Boldyrev, *Phys. Rev. Lett.* **97**, 255002 (2006)
- W.H. Matthaeus, S.L. Lamkin, *Phys. Fluids* **28**, 303 (1985)
- W.H. Matthaeus, S.L. Lamkin, *Phys. Fluids* **29**, 2513 (1986)
- W.H. Matthaeus, D. Montgomery, *Ann. N.Y. Acad. Sci.* **357**, 203 (1980)
- W.H. Matthaeus, A. Pouquet, P.D. Mininni, P. Dmitruk, B. Breech, *Phys. Rev. Lett.* **100**, 085003 (2008a)
- W.H. Matthaeus, S. Servidio, P. Dmitruk, *Phys. Rev. Lett.* **101**, 149501 (2008b)
- H. Meheut, S. Fromang, G. Lesur, M. Joos, P.-Y. Longaretti, *Astron. Astrophys.* (2015, submitted). [arXiv: 1505.05661](https://arxiv.org/abs/1505.05661)
- M. Meneguzzi, H. Politano, A. Pouquet, M. Zolver, *J. Comp. Physiol.* **123**, 32 (1996)
- C. Meneveau, J. Katz, *Annu. Rev. Fluid Mech.* **32**, 1 (2000)
- L.J. Milano, W.H. Matthaeus, P. Dmitruk, D.C. Montgomery, *Phys. Plasmas* **8**, 2673 (2001)
- K. Miki, S. Menon, *Phys. Plasmas* **15**, 072306 (2008)
- M.D. Millionshchikov, *Izv. Akad. Nauk SSSR, Ser. Geogr. Geofiz.* **5**(4–5), 433 (1941)
- P. Mininni, E. Lee, A. Norton, J. Clyne, *New J. Phys.* **10**, 125007 (2008)
- D. Mitra, S. Candelaresi, P. Chatterjee, R. Tavakol, A. Brandenburg, *Astron. Nachr.* **331**, 130 (2010)
- H.K. Moffatt, *Magnetic Field Generation in Electrically Conducting Fluids* (Cambridge University Press, Cambridge, 1978), 353 pp.
- D.C. Montgomery, L. Turner, G. Vahala, *Phys. Fluids* **21**, 757 (1978)
- D.C. Montgomery, L. Turner, *Phys. Fluids* **24**, 825 (1981)
- D.C. Montgomery, *Phys. Scr.* **T2/1**, 83 (1982)
- P. Morel, A. Bañón Navarro, M. Albrecht-Marc, D. Carati, F. Merz, T. Görler, F. Jenko, *Phys. Plasmas* **18**, 072301 (2011)
- P. Morel, A. Bañón Navarro, M. Albrecht-Marc, D. Carati, F. Merz, T. Görler, F. Jenko, *Phys. Plasmas* **19**, 012311 (2012)
- W.-C. Müller, D. Biskamp, *Turbulence and Magnetic Fields in Astrophysics* (Springer, New York, 2003)
- W.-C. Müller, D. Carati, *Phys. Plasmas* **9**, 824 (2002a)
- W.-C. Müller, D. Carati, *Comput. Phys. Commun.* **147**, 344 (2002b)
- W.-C. Müller, S.K. Malapaka, A. Busse, *Phys. Rev. E* **85**, 015302(R) (2012)

- N.J. Nelson, B.P. Brown, A.S. Brun, M.S. Miesch, J. Toomre, *Astrophys. J.* **739**, L38 (2011)
- N.J. Nelson, B.P. Brown, A.S. Brun, M.S. Miesch, J. Toomre, *Astrophys. J.* **762**, 73 (2013)
- A. Nordlund, *Astron. Astrophys.* **107**, 1 (1982)
- A. Nordlund, *Sol. Phys.* **100**, 209 (1985)
- A. Nordlund, R.F. Stein, M. Asplund, *Living Rev. Sol. Phys.* **6**, 2 (2009). <http://www.livingreviews.org/lrsp-2009-2>
- S.A. Orszag, *Fluid Dynamics* (Les Houches Summer School of Theoretical Physics, Les Houches, 1973), p. 237
- S. Oughton, E.R. Priest, W.H. Matthaeus, *J. Fluid Mech.* **280**, 95 (1994)
- S. Oughton, K.H. Rädler, W.H. Matthaeus, *Phys. Rev. E* **56**(3), 2875 (1997)
- R.V. Ozmidov, *Izv., Atmos. Ocean. Phys.* **1**(8), 853 (1965). Translated into English, *Phys. Rev. E* **56**(3), 2875 (1997)
- T.N. Parashar, S. Servidio, B. Breech, M.A. Shay, W.H. Matthaeus, *Phys. Plasmas* **17**, 102304 (2010)
- E.N. Parker, *Astrophys. J.* **174**, 499 (1972)
- E.N. Parker, *Cosmical Magnetic Fields* (Clarendon Press/Oxford University Press, New York, 1979), 858 pp.
- T. Passot, P.L. Sulem, P. Hunana, *Phys. Plasmas* **19**, 082113 (2012)
- R.B. Pelz, V. Yakhot, S.A. Orszag, L. Shtilman, E. Levich, *Phys. Rev. Lett.* **54**, 2505 (1985)
- S. Perri, M.L. Goldstein, J.C. Dorelli, F. Sagraoui, *Phys. Rev. Lett.* **109**, 191101 (2012)
- A. Petrosyan, A. Balogh, M.L. Goldstein, J. Leorat, E. Marsch, K. Petrovay, B. Roberts, R. von Steiger, J.C. Vial, *Space Sci. Rev.* **156**, 135 (2010)
- U. Piomelli, *J. Aerosp. Sci.* **35**, 335 (1999)
- H. Politano, A. Pouquet, *Phys. Rev.* **52**(1), 636 (1995)
- S.B. Pope, *Turbulent Flows* (Cambridge University Press, Cambridge, 2000)
- A. Pouquet, *Plasma Astrophysics*. Series Lecture Notes in Physics, vol. 468 (1996), p. 163
- A. Pouquet, J. Baerenzung, J. Graham Pietarila Graham, P. Mininni, H. Politano, Y. Ponty, Modeling of turbulent flows in the presence of magnetic fields or rotation, in *T12009 Conference (Ste Luce), Notes on Numerical Fluid Mechanics and Multidisciplinary Design*, vol. 110, ed. by M. Deville, J.-P. Sagaut, T. Hiep (2010), p. 287
- A. Pouquet, U. Frisch, J. Léorat, *J. Fluid Mech.* **77**, 321 (1976)
- E. Priest, C.J. Schrijver, *Sol. Phys.* **190**, 1 (1999)
- F. Pucci, M. Velli, *Astrophys. J. Lett.* **780**, LL19 (2014)
- H. Qin, W.M. Tang, W.W. Lee, *Phys. Plasmas* **7**, 4433 (2000)
- E. Quataert, W. Dorland, G.W. Hammett, *Astrophys. J.* **577**, 524 (2002)
- A.F. Rappazzo, M. Velli, G. Einaudi, *Astrophys. J.* **722**, 65 (2010)
- A.F. Rappazzo, W.H. Matthaeus, D. Ruffolo, S. Servidio, M. Velli, *Astrophys. J.* **758**, L14 (2012)
- M.M. Ray, P. Moin, *J. Comp. Physiol.* **96**, 15 (1991)
- M. Rempel, *Astrophys. J.* **789**, 132 (2014), 22 pp.
- H.P. Robertson, *Proc. Camb. Philos. Soc.* **36**, 209 (1940)
- D.C. Robinson, M.G. Rusbridge, *Phys. Fluids* **14**, 2499 (1971)
- P.L. Roe, *Annu. Rev. Fluid Mech.* **18**, 337 (1986)
- I. Rogachevskii, N. Kleeorin, *Phys. Rev. E* **76**, 056307 (2007)
- G. Rüdiger, L.L. Kitchatinov, A. Brandenburg, *Astron. Astrophys.* **269**, 3 (2011)
- P. Sagaut, *Large Eddy Simulation for Incompressible Flows: An Introduction*. Series on Scientific Computation (Springer, Berlin, 2006), 556 pp.
- P. Sagaut, C. Cambon, *Homogeneous Turbulence Dynamics* (Cambridge University Press, New York, 2008)
- R. Samtaney, N.F. Loureiro, D.A. Uzdensky, A.A. Schekochihin, S.C. Cowley, *Phys. Rev. Lett.* **103**, 105004 (2009)
- F. Sagraoui, M.L. Goldstein, P. Robert, Y.V. Khotyaintsev, *Phys. Rev. Lett.* **102**, 231102 (2009)
- F. Sagraoui, M.L. Goldstein, G. Belmont, P. Canu, L. Rezeau, *Phys. Rev. Lett.* **105**, 131101 (2010)
- A. Salhi, T. Lehner, F. Godeferd, C. Cambon, *Phys. Rev. E* **85**, 026301 (2012)
- A. Salhi, F.G. Jacobitz, K. Schneider, C. Cambon, *Phys. Rev. E* **89**, 013020 (2014)
- A.A. Schekochihin, S.C. Cowley, W. Dorland et al., *Astrophys. J. Suppl.* **182**, 310 (2009)
- W. Schmidt, *Living Rev. Comput. Astrophys.* (2015, in press). [arXiv:1404.2483](https://arxiv.org/abs/1404.2483)
- J.F. Scott, *J. Fluid Mech.* **741**, 316–349 (2014)
- N. Seehafer, *Phys. Rev. E* **53**, 1283 (1996)
- S. Servidio, W.H. Matthaeus, P. Dmitruk, *Phys. Rev. Lett.* **100**, 095005 (2008)
- S. Servidio, W.H. Matthaeus, M.A. Shay, P.A. Cassak, P. Dmitruk, *Phys. Rev. Lett.* **102**, 115003 (2009)
- S. Servidio, W.H. Matthaeus, M.A. Shay, P. Dmitruk, P.A. Cassak, M. Wan, *Phys. Plasmas* **17**, 032315 (2010)
- S. Servidio, F. Valentini, F. Califano, P. Veltri, *Phys. Rev. Lett.* **108**, 045001 (2012)
- S. Servidio, K.T. Osman, F. Valentini, D. Perrone, F. Califano, S. Chapman, W.H. Matthaeus, P. Veltri, *Astrophys. J. Lett.* **781**, LL27 (2014)

- Z.S. She, E. Leveque, *Phys. Rev. Lett.* **72**(3), 336 (1994)
- J.V. Shebalin, W.H. Matthaeus, D. Montgomery, *J. Plasma Phys.* **29**, 525 (1983)
- K.R. Sheltnivasan, R.A. Antonia, *Annu. Rev. Fluid Mech.* **29**, 435 (1997)
- D. Smith, S. Ghosh, P. Dmitruk, W.H. Matthaeus, *Geophys. Res. Lett.* **31**, L02805 (2004)
- E.A. Spiegel, *Astron. Astrophys.* **9**, 323 (1971)
- E.A. Spiegel, *Astron. Astrophys.* **10**, 261 (1972)
- J.E. Stawarz, A. Pouquet, M.E. Brachet, *Phys. Rev. E* **86**, 036307 (2012)
- O. Stawicki, S.P. Gary, H. Li, *J. Geophys. Res.* **106**, 8273 (2001)
- M. Steffen, H.-G. Ludwig, S. Krüß, *Astron. Nachr.* **123**, 371 (1989)
- R.F. Stein, A.A. Nordlund, *Astrophys. J.* **342**, L95 (1989)
- R.F. Stein, A.A. Nordlund, *Astrophys. J.* **499**, 914 (1998)
- J.M. Stone, M.L. Norman, *Astrophys. J. Suppl. Ser.* **80**, 753 (1992)
- H.R. Strauss, *Phys. Fluids* **19**, 134 (1976)
- T. Stribling, W.H. Matthaeus, *Phys. Fluids B* **3**, 1848 (1991)
- J.B. Taylor, *Phys. Rev. Lett.* **33**, 1139 (1974)
- J.M. TenBarge, G.G. Howes, W. Dorland, *Astrophys. J.* **774**, 139 (2013)
- A.C. Ting, D. Montgomery, W.H. Matthaeus, *Phys. Fluids* **29**, 3261 (1986)
- S.M. Tobias, F. Cattaneo, S. Boldyrev, MHD dynamos and turbulence, in *Ten Chapters in Turbulence*, ed. by P. Davidson, Y. Kaneda, K.R. Sreenivasan (Cambridge University Press, Cambridge, 2013), 450 pp
- J. Toomre, J.-P. Zahn, J. Latour, E.A. Spiegel, *Astrophys. J.* **207**, 545 (1976)
- N.J. Turner, S. Fromang, C. Gammie, H. Klahr, G. Lesur, M. Wardle, X.-N. Bai, in *Protostars and Planets VI*, ed. by H. Beuther, R. Klessen, C. Dullemond, T. Henning (University of Arizona Press, Tucson, 2014, in press). [arXiv:1401.7306](https://arxiv.org/abs/1401.7306)
- A. Usmanov, M.L. Goldstein, W.H. Matthaeus, *Astrophys. J.* **788**, 43 (2014)
- D.A. Uzdensky, N.F. Loureiro, eprint (2014). [arXiv:1411.4295](https://arxiv.org/abs/1411.4295)
- M. van Noort, L. Rouppe van der Voort, M.G. Lofdahl, *Sol. Phys.* **228** (2005)
- M.K. Verma, *Phys. Rep.* **401**, 229 (2004)
- D. Verscharen, E. March, U. Motschmann, J. Müller, *Phys. Plasmas* **19**, 022305 (2012)
- A. Vögler, Shelyag, M. Schüssler, F. Cattaneo, T. Emonet, *Astron. Nachr.* **429**, 335 (2005)
- S. Wedemeyer, S. Freytag, B. Steffen, M. Ludwig, H.-G. Holweger, *Astron. Nachr.* **414**, 1121 (2004)
- F. Waleffe, *Phys. Fluids A* **4**, 350 (1992)
- M. Wan, S. Oughton, S. Servidio, W.H. Matthaeus, *Phys. Plasmas* **17**, 082308 (2010)
- M. Wan, W.H. Matthaeus, H. Karimabadi et al., *Phys. Rev. Lett.* **109**, 195001 (2012a)
- M. Wan, S. Oughton, S. Servidio, W.H. Matthaeus, *J. Fluid Mech.* **697**, 296 (2012b)
- M. Wan, W.H. Matthaeus, S. Servidio, S. Oughton, *Phys. Plasmas* **20**, 042307 (2013)
- M. Wan, A.F. Rappazzo, W.H. Matthaeus, S. Servidio, S. Oughton, *Astrophys. J.* **797**, 63 (2014)
- P.R. Woodward, D.H. Porter, S. Anderson, T. Fuchs, in *Numerical Modeling of Space Plasma Flows*, ed. by N.V. Pogorelov, G.P. Zank. *ASP Conf. Ser.*, vol. 359 (2006a), pp. 97–110
- P.R. Woodward, D.H. Porter, S. Anderson, T. Fuchs, F. Herwig, *J. Phys. Conf. Ser.* **46**, 370–384 (2006b)
- P. Wu, S. Perri, K. Osman et al., *Astrophys. J. Lett.* **763**, LL30 (2013a)
- P. Wu, M. Wan, W.H. Matthaeus, M.A. Shay, M. Swisdak, *Phys. Rev. Lett.* **111**, 121105 (2013b)
- J.C. Wyngaard, *J. Atmos. Sci.* **61**, 1816 (2004)
- M. Yamada, R. Kulsrud, H. Ji, *Rev. Mod. Phys.* **82**, 603 (2010)
- N. Yokoi, A. Yoshizawa, *Phys. Fluids A* **5**, 464 (1993)
- N. Yokoi, R. Rubinstein, A. Yoshizawa, F. Hamba, *J. Turbul.* **9**, N37 (2008)
- N. Yokoi, K. Higashimori, M. Hoshino, *Phys. Plasmas* **20**, 122310 (2013)
- N. Yokoi, *Geophys. Astrophys. Fluid Dyn.* **107**, 114 (2013)
- A. Yoshizawa, *Phys. Fluids* **30**, 1089 (1987)
- T.A. Zang, R.B. Dahlburg, J.P. Dahlburg, *Phys. Fluids A* **4**(1), 127 (1992)
- G.P. Zank, W.H. Matthaeus, *J. Plasma Phys.* **48**, 85 (1992)
- O. Zeman, *Phys. Fluids* **6**, 3221 (1994)
- V. Zhdankin, D.A. Uzdensky, J.C. Perez, S. Boldyrev, *Astrophys. J.* **771**, 124 (2013)
- V. Zhdankin, D.A. Uzdensky, S. Boldyrev, *Phys. Rev. Lett.* **114**, 065002 (2015)
- Y. Zhou, G. Vahala, *J. Plasma Phys.* **45**, 239 (1991)
- Y. Zhou, W.H. Matthaeus, P. Dmitruk, *Rev. Mod. Phys.* **76**, 1015 (2004)
- S.J. Zweben, C.R. Menyuk, R.J. Taylor, *Phys. Rev. Lett.* **42**, 1720 (1979)
- E.G. Zweibel, M. Yamada, *Annu. Rev. Astron. Astrophys.* **47**, 291 (2009)